

Quantifying the Impact of Global Warming on Saltwater Intrusion at Shelter
Island, New York Using a Groundwater Flow Model

A Final Report Presented

by

Daniel James Rozell

to

The Graduate School

in Partial fulfillment of the

Requirements

for the Degree of

Master of Science

in

Geosciences with concentration in Hydrogeology

Stony Brook University

December, 2007

Stony Brook University

The Graduate School

Daniel James Rozell

We, the Final Report committee for the above candidate for the
Master of Science in Geosciences with concentration in Hydrogeology degree,
Hereby recommend acceptance of this Final Report.

Teng-fong Wong, Research Advisor, Professor,
Department of Geosciences

Gilbert Hanson, Professor,
Department of Geosciences

Henry Bokuniewicz, Professor,
School of Marine and Atmospheric Sciences

Abstract

In order to quantify the effects global warming may have on a small island, a previously published single density steady-state groundwater flow model for Shelter Island, NY was changed to a variable density transient groundwater flow model. The original model code, created for MODFLOW, was adapted to SEAWAT-2000.

The 2007 IPCC report predictions for changes in precipitation and sea level rise over the next century were applied to the calibrated model. A scenario most favorable to groundwater retention consisting of a predicted precipitation increase of 15% and a sea level rise of 0.6 ft was compared to the current long-term average. This resulted in a seaward movement of the interface by an average of 76 ft and a maximum of 199 ft. The water table rose by an average of 0.89 feet. A second scenario least favorable to groundwater retention consisting of a predicted precipitation decrease of 2% and a sea level rise of 2 ft was compared to the current long-term average. This resulted in a landward movement of the interface by an average of 53 ft and a maximum of 121 ft. The water table rose by an average of 1.94 feet.

Table of Contents

LIST OF FIGURES	V
LIST OF TABLES	VI
ACKNOWLEDGEMENTS.....	VII
INTRODUCTION AND OBJECTIVE	1
INTRODUCTION.....	1
OBJECTIVE	3
BACKGROUND.....	4
THEORY.....	4
STUDY AREA.....	10
PREVIOUS MODELS	15
GROUNDWATER FLOW MODEL.....	19
MODEL OVERVIEW.....	19
<i>Model Geometry</i>	19
<i>Boundary Conditions</i>	20
<i>Seawater</i>	24
<i>Recharge</i>	25
<i>Geologic Parameters</i>	26
<i>Pumping</i>	27
<i>Other Assumptions</i>	28
CALIBRATION	29
SENSITIVITY ANALYSIS	36
VALIDATION.....	37
RESULTS.....	39
DISCUSSION	46
CONCLUSION.....	52
FUTURE WORK.....	53
REFERENCES.....	55
APPENDIX 1	60
APPENDIX 2	61

List of Figures

Figure 1: A small island aquifer where the shaded area is the freshwater lens, h represents the water table height above sea level, and z represents the depth of the freshwater/saltwater interface below sea level (modified from Urbano, 2001).....	4
Figure 2: A) Idealized freshwater/saltwater interface under hydrostatic conditions.	6
Figure 3: Location of Shelter Island (Simmons, 1986).....	10
Figure 4: Shelter Island (NY GIS, 2007).....	11
Figure 5: North (A) to South (A') hydrogeologic cross-section of Shelter Island (Simmons, 1986).....	12
Figure 6: Diagram of Shelter Island hydrology where the freshwater lens is deformed by a confining clay layer (Simmons, 1986).....	13
Figure 7: Water table contour map of Shelter Island. The transect C-C' is used in the Schubert (1999) model and the model constructed for this study (modified from Schubert, 1999).	14
Figure 8: Cross section C-C' shows geologic units, freshwater/saltwater interface, and boreholes during March 17-20, 1995 (modified from Schubert, 1999).....	16
Figure 9: Grid spacing for the finite-difference model created from cross-section C-C' (modified from Schubert, 1999)	20
Figure 10: Model boundary conditions from Schubert (1999) study	22
Figure 11: Boundary Conditions for initial model. Grey areas are no-flow cells. Blue cells are constant head boundaries.....	23
Figure 12: Boundary conditions for SEAWAT-2000 model. Orange cells represent constant head boundaries. Grey cells represent saltwater concentrations of 2.18 lbs/ft ³ . ..	23
Figure 13: Boundary conditions for second SEAWAT-2000 model. Orange cells represent constant head. Light grey cells represent saltwater concentrations of 2.18 lbs/ft ³ . Dark grey cells represent the Pleistocene marine clay layer (inactive).	24
Figure 14: Head value scatter diagram from PEST forward run.	33
Figure 15: Head-Time curve for the initial SEAWAT-2000 model showing head levels reach steady state in 350,000 days. Vertical axis units are feet and horizontal units are days.	34
Figure 16: Head-Time curve for the revised SEAWAT-2000 model showing head levels reach steady state in 10,000 days. Vertical axis units are feet and horizontal units are days.	35
Figure 17: Uniform horizontal grid spacing of 50 ft used in grid sensitivity analysis.	37
Figure 18: Reconstructed Schubert model run using PMWIN. Contours show head levels in feet.	39
Figure 19: Transient SEAWAT-2000 model run to steady-state. Contours show head levels in feet.	40
Figure 20: Transient SEAWAT-2000 model run to steady-state. Contours show salt concentration in 10% increments from freshwater to seawater.	40
Figure 21: Revised SEAWAT-2000 model where the marine clay unit is treated as a no-flow boundary. Contours show head levels in feet.	40
Figure 22: Revised SEAWAT-2000 model where the marine clay unit is treated as a no-flow boundary. Contours show salt concentration in 10% increments from freshwater to seawater.....	41

Figure 23: Relative velocity vector field for revised SEAWAT-2000 model. The arrow size in each cell is proportional to the flow velocity and points in the direction of flow. 41

Figure 24: Flow path lines for revised SEAWAT-2000 model. 41

Figure 25: Position of the Freshwater/Saltwater interface in West Neck Bay for three climate change scenarios. All distances are in feet. The interface is defined as an isochlor of 250 mg/L (0.0156 lb/ft³). MSL is the mean sea-level for 2007. The horizontal position of the shoreline is assumed to be stationary in all scenarios. 44

Figure 26: Zone of diffusion for freshwater/saltwater interface for Scenario 1 (top), Scenario 2 (middle), and Scenario 3 (bottom). Axes are in feet and color coded salt concentrations are in lbs /cubic ft. Note that the horizontal axis is not linear. 45

List of Tables

Table 1: Contributing factors to sea level rise (modified from IPCC, Feb. 2007) 1

Table 2: National Geodetic Vertical Datum (NGVD) and mean sea-level within Peconic Bay. All values are in feet (modified from Schubert, 1999). 24

Table 3: Defined geologic units and parameters used in O'Rourke(2000) model. 26

Table 4: Defined geologic units and parameters used in Schubert (1999) model. Conductivities varied slightly at borders between hydrogeologic units. 27

Table 5: Measured and simulated water levels measured in feet above National Geodetic Vertical Datum of 1929 for Schubert (1999) model. (modified from Schubert, 1999)... 30

Table 6: Initial Head Conditions for first model run 30

Table 7: Parameters used for each geologic unit in revised SEAWAT-2000 model. Conductivities varied slightly at borders between hydrogeologic units. 35

Table 8: PEST Parameter Sensitivity Analysis..... 36

Table 9: PEST Observation Sensitivity Analysis 36

Table 10: Comparison of the calibration and validation process results. Precipitation data comes from the Greenport station (see Appendix I). Well head data were taken from March of the following year for modeling consistency. 38

Acknowledgements

I would like to thank Prof. Teng-fong Wong, my advisor, for guiding me to important resources, making helpful suggestions, and encouraging my progress. Additionally, I owe my gratitude to Prof. Hanson and Prof. Bokuniewicz for their time and efforts. I would also like to recognize Jonathan Wanlass of the Suffolk County Department of Health and Margaret Phillips of the U.S. Geological Survey for providing me with data essential to this project. Lastly, I would like to thank Loretta Budd, the Department of Geosciences graduate program coordinator, who has helped me sail smoothly through the sea of paperwork that unavoidably accompanies graduate school.

Introduction and Objective

Introduction

There is considerable public concern and scientific uncertainty regarding the scope and magnitude of the climate change trend popularly called Global Warming. The current general consensus in the scientific community is that anthropogenic sources are causing the Earth to warm and this trend is likely to continue for at least several decades regardless of any mitigating countermeasures taken by humans (IPCC, Feb. 2007). Considerable effort has been expended to quantifiably predict what environmental effects are to be expected over the next century from global warming.

Sea level rise is one of the most often cited effects of global warming. Rising mean sea levels around the world have been documented over the last half century and are hypothesized to be primarily caused by thermal expansion of warming water and melting of glaciers and ice sheets (Table 1). As global warming continues over the next century, mean sea levels will also continue to rise (IPCC, Feb. 2007).

Table 1: Contributing factors to sea level rise (modified from IPCC, Feb. 2007)

Source of sea level rise	Rate of sea level rise (m per century)	
	1961 – 2003	1993 – 2003
Thermal expansion	0.042 ± 0.012	0.16 ± 0.05
Glaciers and ice caps	0.050 ± 0.018	0.077 ± 0.022
Greenland ice sheets	0.05 ± 0.12	0.21 ± 0.07
Antarctic ice sheets	0.14 ± 0.41	0.21 ± 0.35
Sum of individual climate contributions to sea level rise	0.11 ± 0.05	0.28 ± 0.07
Observed total sea level rise	0.18 ± 0.05^a	0.31 ± 0.07^a
Difference (Observed minus sum of estimated climate contributions)	0.07 ± 0.07	0.03 ± 0.10

Note:

^a Data prior to 1993 are from tide gauges and after 1993 are from satellite altimetry

Rising sea levels are of particular concern to small islands. These areas are extremely vulnerable to sea level fluctuations for several reasons. First, many small islands have a large portion of their land mass at low elevation. For example, Kiribati, Tuvalu, the Marshall Islands, and the Maldives, have no ground more than 4 meters above mean sea level (WMO, 2005). Thus, any rise in sea level can cause a considerable percentage of the island to be submerged. Additionally, because of their limited area, the freshwater stored as surface streams and lakes or as groundwater is likewise limited.

Islands which use surface water to supply inhabitants with potable water have the difficult task of maintaining a barrier between the surface water and rising sea water. However, attempting to prevent saltwater contamination of groundwater is an even more daunting endeavor. Thus, islands which are completely dependent on their groundwater as a source of fresh water, such as Pacific atoll islands or Caribbean limestone islands, are further at risk of losing an adequate potable water supply due to saltwater intrusion created by rising sea levels (WMO, 2005). For small island developing states, the risks of sea level rise are compounded by their limited economic and political resources which hamper their ability to mitigate the effects of global warming on their inhabitants and natural resources.

Unlike seawater inundation of land, saltwater intrusion of a groundwater aquifer is more difficult to quantify because of a variety of additional factors involved. While submersion of land is dependent only on the land elevation and the amount of sea level rise, saltwater intrusion is also dependent upon local geologic conditions, groundwater pumping, and changes in recharge due to variable precipitation and evapotranspiration rates.

Objective

The intent of this study is to further investigate the relationship between climate change and saltwater intrusion in a small island aquifer. This study applies the climate and sea level rise estimates of the Intergovernmental Panel on Climate Change (IPCC) Fourth Assessment Report (AR4) published in 2007 to a finite-difference groundwater flow model of Shelter Island, New York, a small island whose inhabitants are dependent on the island's freshwater lens for potable water. The study consists of constructing a reliable groundwater model of Shelter Island's aquifer that includes a variable freshwater/saltwater interface, applying the AR4 predictions of sea level and recharge changes, and using the model to predict changes in saltwater intrusion into the groundwater system. The findings of this study could be used by the residents of Shelter Island to make informed long-term water resource management decisions. More generally, the methods and results of this study may be of value to similar small inhabited islands that need to plan for future fresh water requirements.

Background

Theory

Seawater's high salinity results in a density approximately 2.5% greater than freshwater. This density difference is large enough to prevent substantial mixing between the freshwater and saltwater. Thus, a typical freshwater aquifer on a small island resembles a lens floating on saltwater as seen in Figure 1. Although this interface is often represented as sharp and impermeable, it actually exists as a zone of diffusion with the freshwater boundary delineated by some defined chloride concentration, often a potable water standard (Domenico and Schwartz, 1998).

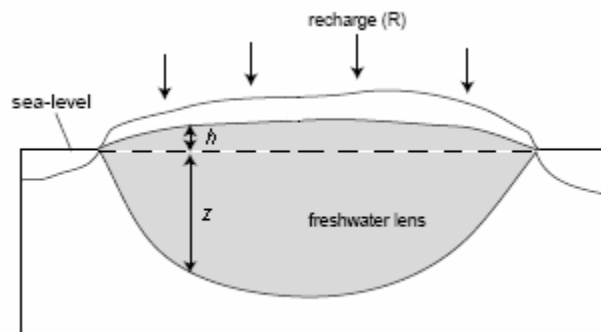


Figure 1: A small island aquifer where the shaded area is the freshwater lens, h represents the water table height above sea level, and z represents the depth of the freshwater/saltwater interface below sea level (modified from Urbano, 2001)

The depth of the interface between fresh and saline water near a shore was first empirically determined independently by Baden-Ghyben (1889) and Herzberg (1901) to be 40 times the height of the water table when referenced against mean sea level. The analytic explanation of this phenomenon, referred to as the Ghyben-Herzberg formula, is based on a hydrostatic water column of freshwater overlaying saltwater with an impermeable interface (Domenico and Schwartz, 1998). The weight of the freshwater

column, $(h + z)g \rho_f$, is balanced by the weight of a saltwater column, $zg \rho_s$. Set equal to each other and rearranged, the resulting equation is:

$$z = h \frac{\rho_f}{(\rho_s - \rho_f)} \quad (1)$$

where h is the height of the freshwater column above sea level, z is the depth of the interface below sea level, ρ_f is the density of freshwater, and ρ_s is the density of saltwater. Substituting in the average relative densities of fresh and salt water, 1 and 1.025, the Ghyban-Herzberg formula simplifies to

$$z = 40h \quad (2)$$

which corresponds to the original empirical data. However, this simple hydrostatic analysis does not take groundwater discharge to sea into account so it only roughly approximates the actual position of the freshwater/saltwater interface (Figure 2A).

Taking freshwater subsurface discharge into account, such as the Glover (1959) solution for a confined aquifer or the Rumner Jr. and Shiau (1968) solution for an unconfined aquifer, results in a more realistic saltwater interface as seen in Figure 2B.

The Rumner Jr. and Shiau (1968) analytical solution, which applies to the aquifer in this study (Paulsen et al, 2004), defines the flow net near the interface between salt and fresh water by a set of coordinates (X,Z) given by the following equations:

$$X = \frac{Q}{\sqrt{K_x K_z}} \frac{K_x}{K_z} \left[\frac{(G+1)}{2} (\Phi^2 - \Psi^2) - \Psi \right] \quad (3a)$$

$$Z = \frac{Q}{\sqrt{K_x K_z}} \frac{K_x}{K_z} [(G+1)\Phi\Psi + \Phi] \quad (3b)$$

where X is the horizontal position of the interface measured inland from the shoreline, Z is the depth of the interface measured from the intersection of the water table and land

surface, Q is the discharge per unit width of the aquifer, K_x and K_z are the horizontal and vertical hydraulic conductivities of the aquifer, and the density contrast parameter, G , is defined as:

$$G = \frac{\rho_f}{(\rho_s - \rho_f)} \quad (3c)$$

Also, the potential function, Φ , is

$$\Phi = -\frac{K_z h}{Q} \quad (3d)$$

and Ψ is the stream function such that $\Psi = -1$ represents the freshwater/saltwater interface.

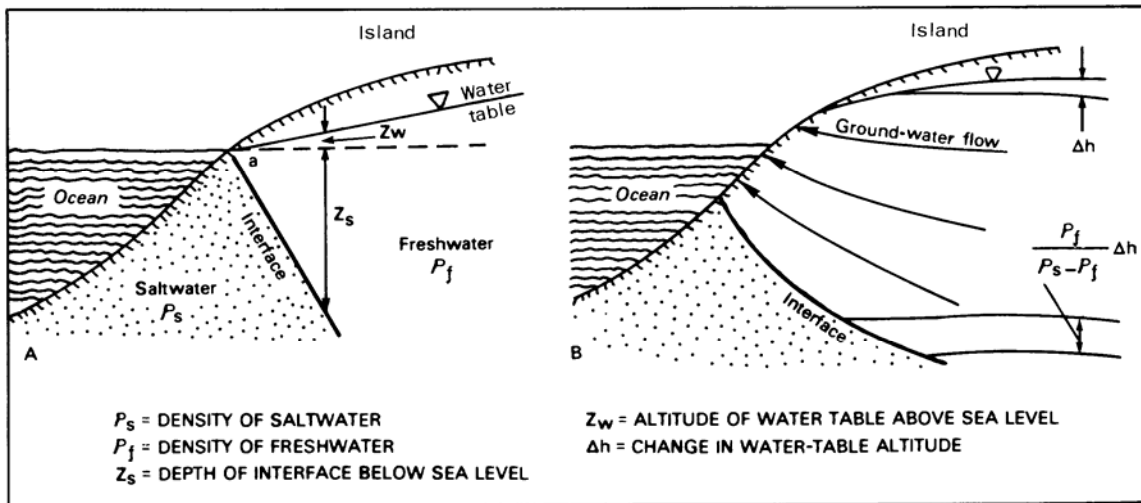


Figure 2: A) Idealized freshwater/saltwater interface under hydrostatic conditions.
 B) Freshwater/saltwater interface that includes discharge of groundwater to the sea
 (modified from Freeze and Cherry, 1979)

If sea level rises due to climate change, the position of the freshwater/saltwater interface, as defined by the Rumer Jr. and Shiau equations, will shift inland and upwards as the origin, (X_0, Z_0) moves inland and to higher elevation. Likewise, assuming higher

evapotranspiration rates and lowered recharge, the depth of the freshwater/saltwater interface, Z , should decrease as discharge, Q , decreases.

Although analytical solutions effectively model simple theoretical scenarios, numerical methods allow for complex, irregular, and heterogeneous scenarios to be modeled. The most widely used groundwater flow numerical modeling program is the USGS program MODFLOW, originally documented by McDonald and Harbaugh (1984), which uses finite-difference methods to simulate three-dimensional groundwater flows (Harbaugh et al., 2000). Within a defined grid of cells, MODFLOW iteratively solves the following partial differential equation for the node in each cell (McDonald and Harbaugh, 1988):

$$\frac{\partial}{\partial x} \left(K_{xx} \frac{\partial h}{\partial x} \right) + \frac{\partial}{\partial y} \left(K_{yy} \frac{\partial h}{\partial y} \right) + \frac{\partial}{\partial z} \left(K_{zz} \frac{\partial h}{\partial z} \right) + W = S_s \frac{\partial h}{\partial t} \quad (4)$$

where K_{xx} , K_{yy} , and K_{zz} are values of hydraulic conductivity along the x, y, and z coordinate axes, which are assumed to be parallel to the major axes of hydraulic conductivity; h is the potentiometric head; W is a volumetric flux per unit volume representing sources and/or sinks of water, with $W < 0$ for flow out of the ground-water system, and $W > 0$ for flow in; S_s is the specific storage of the porous material; and t is time.

Equation (4) assumes constant density fluid, so it cannot be used to model saltwater intrusion. As a result, SEAWAT was developed to model variable-density flows (Langevin et al., 2003). SEAWAT-2000, the version used in this study, is based on MODFLOW-2000 (Harbaugh et al., 2000) and MT3DMS (Zheng and Wang, 1999), a solute transport application. Within a defined grid of cells, SEAWAT iteratively solves

the following partial differential equation for the node in each cell (Guo and Langevin, 2002):

$$\begin{aligned} & \frac{\partial}{\partial \alpha} \left[\rho K_{f\alpha} \left(\frac{\partial h_f}{\partial \alpha} + \frac{\rho - \rho_f}{\rho_f} \frac{\partial Z}{\partial \alpha} \right) \right] + \frac{\partial}{\partial \beta} \left[\rho K_{f\beta} \left(\frac{\partial h_f}{\partial \beta} + \frac{\rho - \rho_f}{\rho_f} \frac{\partial Z}{\partial \beta} \right) \right] \\ & + \frac{\partial}{\partial \gamma} \left[\rho K_{f\gamma} \left(\frac{\partial h_f}{\partial \gamma} + \frac{\rho - \rho_f}{\rho_f} \frac{\partial Z}{\partial \gamma} \right) \right] + \rho_s q_s = \rho S_f \frac{\partial h_f}{\partial t} + \theta \frac{\partial \rho}{\partial C} \frac{\partial C}{\partial t} \end{aligned} \quad (5)$$

where α, β, γ are orthogonal coordinate axes, aligned with the principal directions of permeability; t is time; θ is effective porosity; C is solute concentration; ρ is the density of the native aquifer water; ρ_f is the density of freshwater; Z is the elevation at the measurement point; ρ_s is fluid density of source or sink water; and q_s is the volumetric flow rate of sources and sinks per unit volume of aquifer. Additionally, K_f is equivalent freshwater hydraulic conductivity which is defined as:

$$K_{f\alpha} = \frac{k_\alpha \rho_f g}{\mu_f} \quad (6)$$

where k_α is the measured hydraulic conductivity in the α direction, g is the acceleration due to gravity, and μ_f is the viscosity of freshwater under standard conditions (Guo and Langevin, 2002). Likewise, S_f is equivalent freshwater specific storage which is defined as:

$$S_f = S \rho_f g \quad (7)$$

where S is the aquifer specific storage.

Equation (5) is expressed in terms of equivalent freshwater head, i.e., the higher head level that would occur in a piezometer if the saline water in the column were replaced with fresh water. This is done solely for simplifying calculations and does not

necessarily represent a real measurement method. In the original SEAWAT program, the user was required to manually convert all input head values measured in seawater to equivalent freshwater heads and convert all output back from equivalent freshwater heads. However, SEAWAT-2000 internally converts between actual head readings and equivalent freshwater heads using (Langevin et al., 2003):

$$h_f = \frac{\rho}{\rho_f} h - \frac{\rho - \rho_f}{\rho_f} Z \quad (8)$$

and

$$h = \frac{\rho_f}{\rho} h_f + \frac{\rho - \rho_f}{\rho_f} Z \quad (9)$$

Comparing Equations (4) and (5): the first three terms on the left-hand side of each equation represent the net flux across the unit volume's faces, the fourth left-hand side term represents the flux from sources and sinks within the unit volume, and the first term on the right-hand side of each equation represents the time rate of change of water stored within the unit volume. The only important distinction is that Equation (4) uses volumetric fluxes whereas Equation (5) uses mass fluxes in order to account for variable density. The second right-hand term in Equation (5), which has no corresponding term in Equation (4), represents the rate of fluid mass change caused by a solute concentration change. If there is no solute change and density remains constant, this term equals zero and Equations (4) and (5) become functionally equivalent.

In the case of saltwater intrusion simulations, variable-density flow is coupled with solute transport and density changes are assumed to be wholly dependent on solute concentration (i.e. temperature and pressure are ignored). This relationship is defined as:

$$\rho = \rho_f + \frac{\partial \rho}{\partial C} C \quad (10)$$

and the user must supply values for ρ_f , the density of freshwater, and $\partial \rho / \partial C$, typically set to 0.7143 for standard freshwater/saltwater simulations (Langevin et al., 2003).

Study Area

Shelter Island, New York is located on the eastern end of Long Island in Peconic Bay (Figure 3). The island has an area of 12 mi² and, like many small islands, has very little fresh surface water (Soren, 1978) (Figure 4). According to the 2000 US Census, Shelter Island's population is 2,228, but summer seasonal population exceeds 10,000 (Simmons, 1986). The inhabitants are dependent on the island's freshwater lens as a source of potable water.

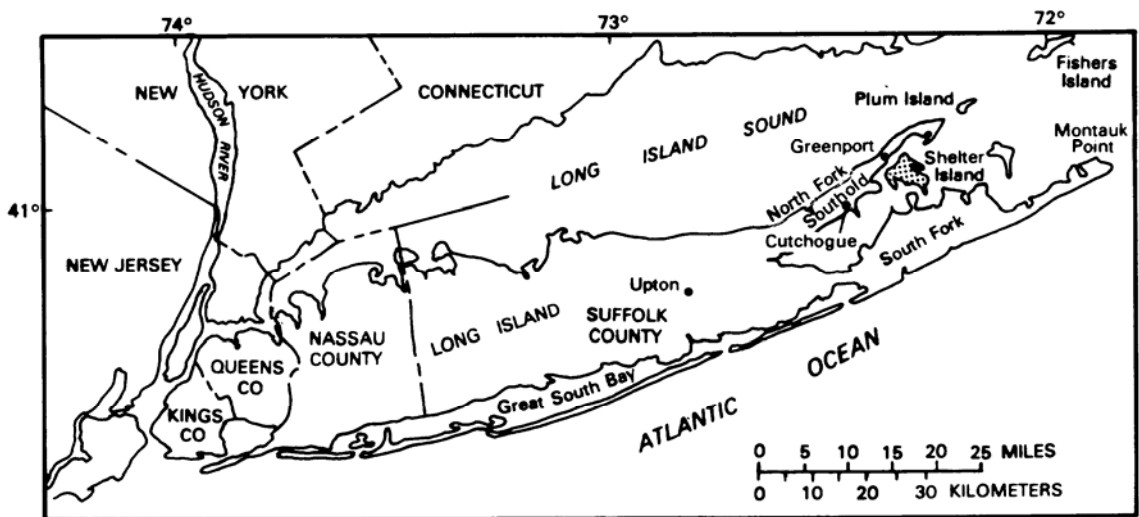


Figure 3: Location of Shelter Island (Simmons, 1986)

The geology of Long Island was first described by Fuller (1914) and the hydrology by Veatch et al. (1906). More recent large hydrology studies were conducted by Cohen et al. (1968), Franke and McClymonds (1972), and Nemickas et al. (1989). In a hydrogeologic investigation of Shelter Island conducted by Soren (1978), fresh

groundwater was found to be restricted to the thin sand and gravel deposits of the Upper Glacial aquifer and that this geological layer is susceptible to saltwater intrusion. In the Soren study, 17 monitoring wells were installed throughout Shelter Island and data was collected starting in June, 1974. Although northern sections of the island have elevations over 100 ft, it was found that the water table rarely exceeds 5 ft above sea level.

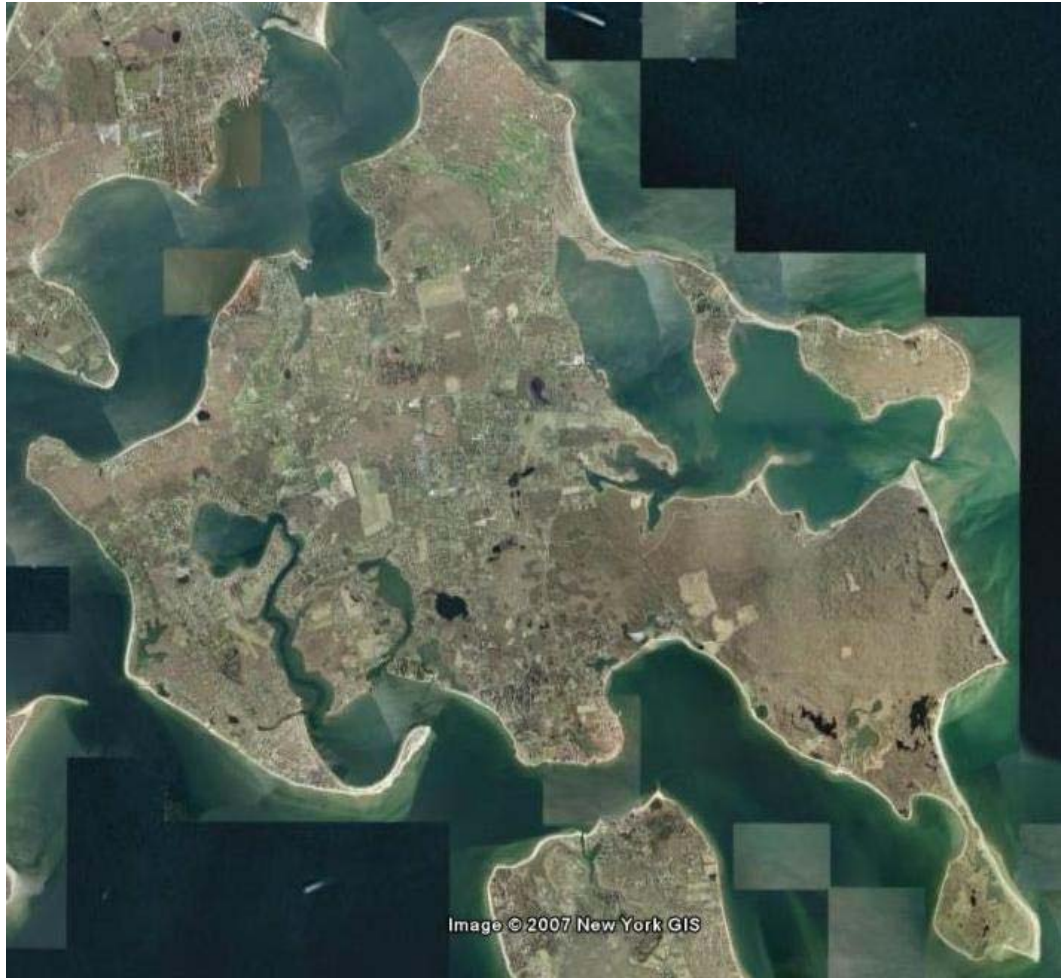


Figure 4: Shelter Island (NY GIS, 2007)

Likewise, ponds and marshes form primarily in depressions less than 5 ft above sea level and there are no significant streams on the island. Figure 5 shows a vertical section of the proposed hydrogeologic conditions. A Pleistocene marine clay layer

deposit 65 ft to 100 ft below sea level marks the lower boundary of the fresh water aquifer (Soren, 1978).

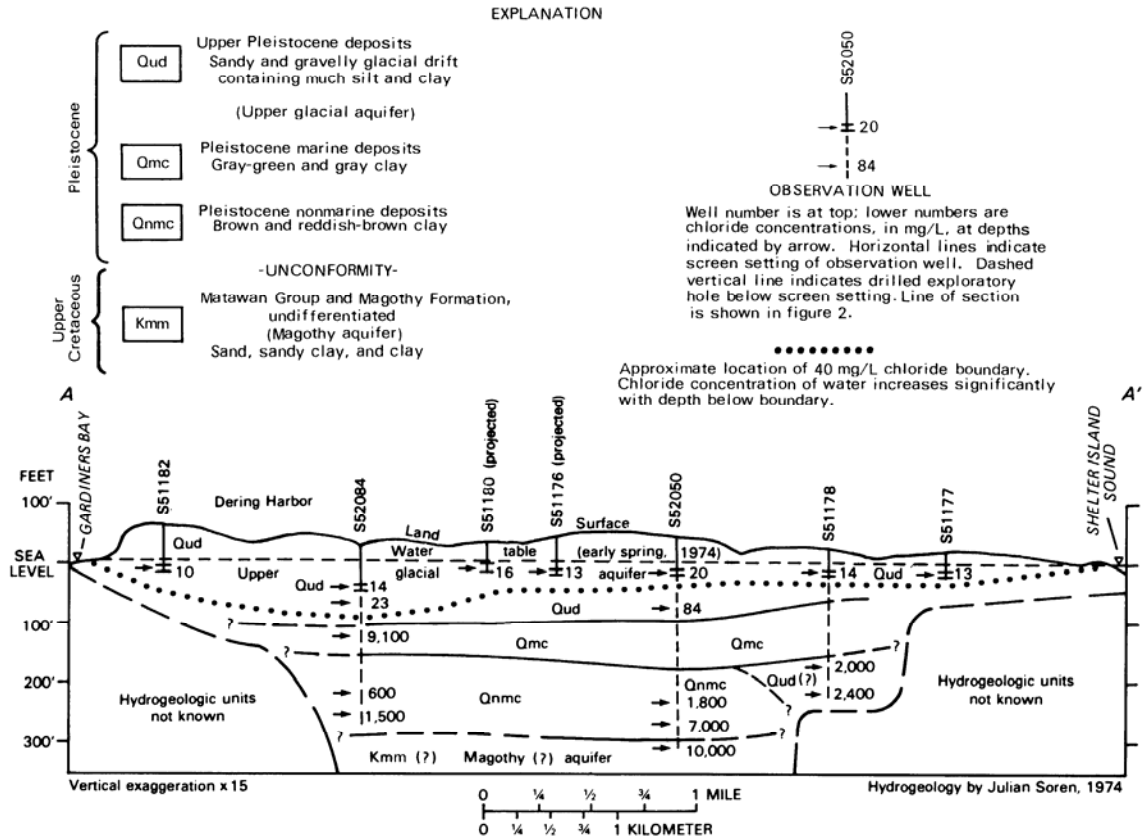


Figure 5: North (A) to South (A') hydrogeologic cross-section of Shelter Island (Simmons, 1986)

A subsequent study by Simmons (1986) added an additional 10 monitoring wells in 1983. Measurements of chloride concentrations showed that the saltwater zone of diffusion moves seasonally. The water table is highest in early spring and lowest at the end of summer where some near shore areas have less than 20-ft of freshwater below them. Additionally, it was found that monthly variations in precipitation affected water-table fluctuations more than any climatic trends from 1974-1983 (Simmons, 1986). Also,

precipitation and evapotranspiration are the main components affecting aquifer recharge; less than 1% of precipitation becomes overland runoff (Nemickas and Koszalka, 1982).

The position of the marine clay layer beneath Shelter Island tends to deform the island's freshwater lens (see Figure 6), preventing upconing, but increasing the lateral movement of saltwater within the Upper Glacial aquifer. Thus, the saltwater interface deviates substantially from the Ghyben-Herzberg approximation (Simmons, 1986).

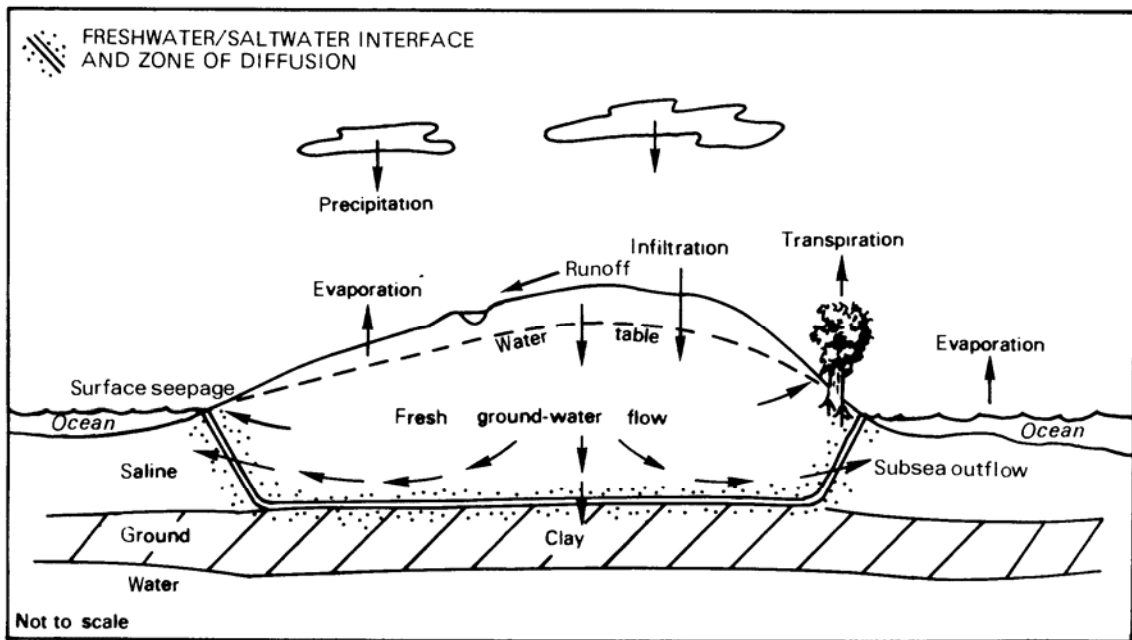
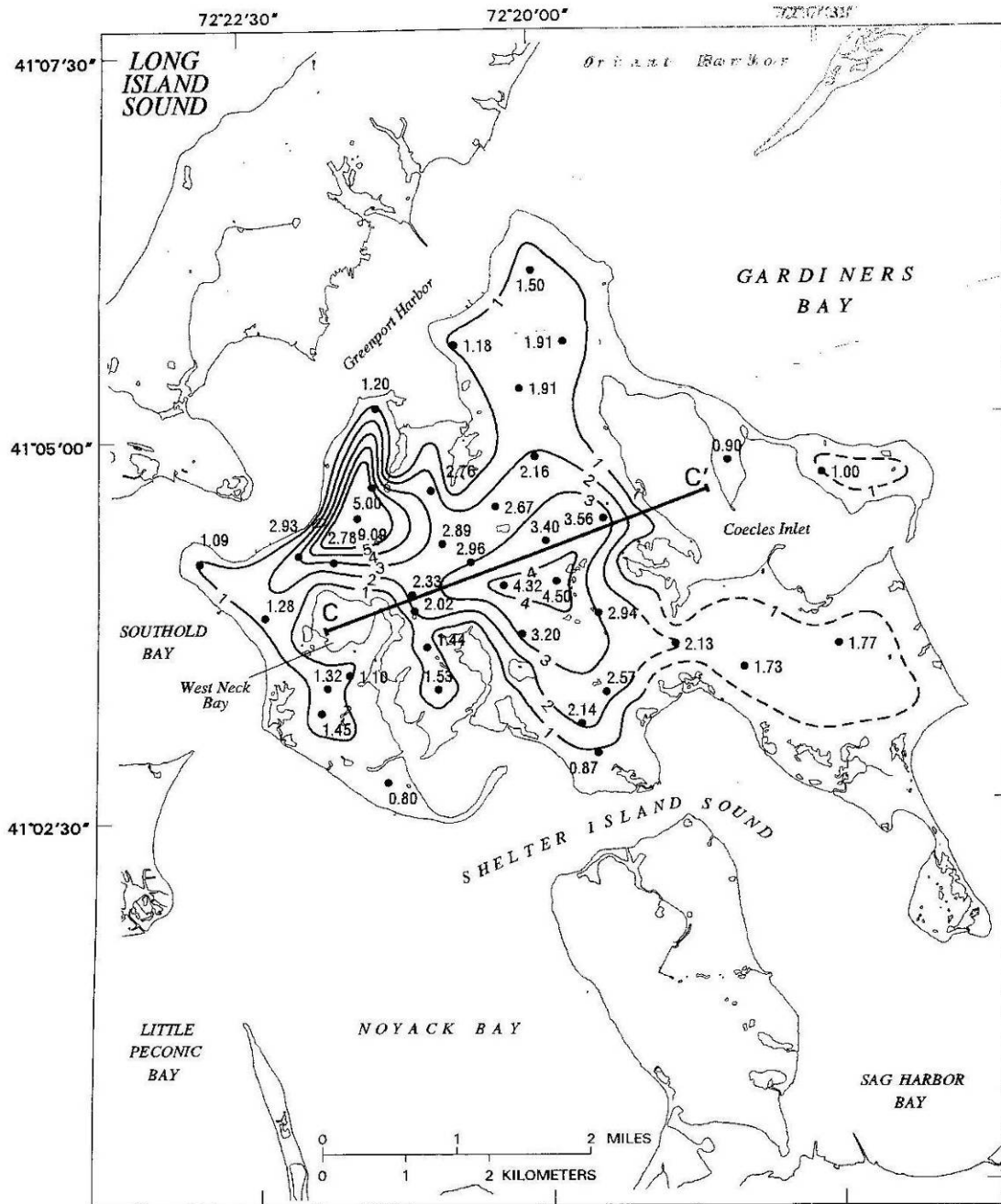


Figure 6: Diagram of Shelter Island hydrology where the freshwater lens is deformed by a confining clay layer (Simmons, 1986)

A groundwater budget performed by Schubert (1998) determined that groundwater discharge from Shelter Island to the surrounding Peconic Estuary was 1.72 million ft³/day. Also, water-table mapping indicated that the island's irregular water table has two mounds and that groundwater generally flows radially outward to the surrounding shoreline (Figure 7). For near-shore wells influenced by tidal variation, head measurements were typically made within 1-hour of high tide when the rate of change was smallest (Schubert, 1999)



Base from U.S. Geological Survey digital data

EXPLANATION

- C — C' LINE OF SECTION — Shows trace of vertical section shown in figure 4C.
- 1 — WATER-TABLE CONTOUR — Shows altitude of water table on March 17-20, 1995. Dashed where approximately located. Contour interval 1 foot. Datum is sea level.
- 1.77 OBSERVATION WELL — Number indicates altitude of water, in feet above sea level.

Figure 7: Water table contour map of Shelter Island. The transect C-C' is used in the Schubert (1999) model and the model constructed for this study (modified from Schubert, 1999).

Previous Models

Buxton and Modica (1992) created one of the first computer groundwater flow models for Long Island. Schubert (1999) created a groundwater flow model for Shelter Island simulating a two-dimensional vertical section across Shelter Island in order to determine groundwater distribution, flow paths, and groundwater travel time (Figure 7). Borehole data was used to map the hydrogeologic characteristics of the vertical section (Figure 8). Schubert found that almost all recharge left the groundwater system as shoreline underflow with an average flow age of less than 20 yrs. The small amount that traveled through the Pleistocene marine clay layer and emerged as sub-sea underflow had an average age of about 1,800 yrs.

A three-dimensional groundwater flow model of Shelter Island was created by O'Rourke (2000) with the purpose of quantifying coastal groundwater discharge into West Neck Bay of Shelter Island and comparing results to field data. The model computed monthly average specific discharges into West Neck Bay ranging from 0.64 ft/day to 0.84 ft/day while field measurements yielded monthly average specific discharges ranging from 0.44 ft/day to 1.49 ft/day.

In a closely related study by Paulsen et al. (2004), field measurements of submarine groundwater discharge into West Neck Bay were taken at three sites, all within close proximity to the western end of the Shelter Island cross-section modeled by Schubert (1999). In that study, data from a borehole 295 ft inland indicated that the freshwater/saltwater interface was at 68 ft below sea level with fine sand from surface to 97 ft below sea level and marine gray clay from 97 ft to 110 ft. Submarine groundwater discharge was found to range from 0.07 to 7.4 ft/day depending on location and tide.

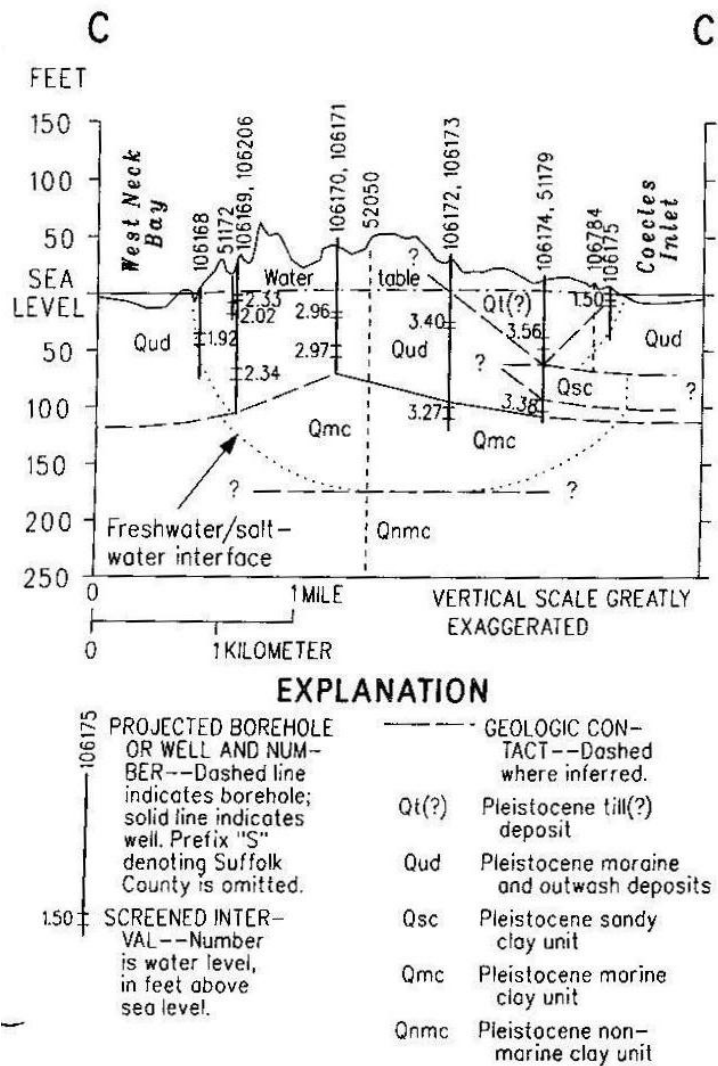


Figure 8: Cross section C-C' shows geologic units, freshwater/saltwater interface, and boreholes during March 17-20, 1995 (modified from Schubert, 1999)

Urbano (2001) modeled the effects of climate change on a freshwater aquifer using a finite-difference model. The study area, Nantucket Island, Massachusetts, has very similar geologic and climatic conditions to Shelter Island (Pearson et al., 1998). The study used estimates from the US Global Change Research Program that predicted groundwater recharge in the northeastern US would range from -30% to +20% in the year 2100 (NAST, 2000). Likewise, from the IPCC 2001 Third Assessment Report, mean sea level in 2100 was predicted to rise between 20 and 90 cm at a rate of 5 mm/year (IPCC

WGII , 2001). The Urbano (2001) model predicted that a 5% reduction in recharge created a 20% increase in the rate of saltwater intrusion. Similarly, a 5 mm/yr sea level rise created an 8% increase in the rate of saltwater intrusion.

Tiruneh and Motz (2003) used SEAWAT to model the movement of the freshwater/saltwater interface in a coastal aquifer that was influenced by global warming. The study used six different climate change scenarios described in the 2001 IPCC Third Assessment Report as inputs to a model that represented an idealized coastal aquifer with inland pumping wells. After 100 years, compared to a scenario with no pumping or sea level rise, a scenario with pumping showed a 2% salinity increase, a scenario with sea level rise showed a 9% increase, and a scenario with both showed a 12% increase.

Misut et al. (2004) used the USGS quasi-three-dimensional finite-difference program SHARP to simulate saltwater intrusion in the North Fork of Long Island due to pumping and drought. One of the scenarios modeled was a 5-year drought that consisted of a 20% recharge reduction below the average (1959-1999) recharge rate and a 20% increase in agricultural pumping over 1999 rates. Simulation results found saltwater intrusion risk at 6 out of 10 wells and an average upward movement of the freshwater/saltwater interface of several feet.

The hydrogeologic conditions of the North Fork of Long Island are similar to Cape Cod, Massachusetts (Schubert, 1999). Masterson (2004) used SEAWAT to model the effects of pumping, decreases in recharge, and sea level rise on four freshwater lenses in Lower Cape Cod, Massachusetts. A rising sea level in model simulations caused water tables to rise, stream flows to increase, and a decrease in the depth of freshwater/saltwater interfaces. Due to the increased stream flow, the simulated water table rose slower than

local sea-level. This resulted in the thinning of the aquifer. Neither field data nor model simulations indicated that the freshwater/saltwater interface moved with seasonal changes in recharge. Only multi-year changes caused substantial movement of the interface within the model. Masterson and Garabedian (2007) used the same model to show that a 2.65 mm/yr sea level rise between 1929 and 2050 causes a freshwater lens thickness decrease of 2% away from streams and 22% to 31% near streams.

Groundwater Flow Model

Model Overview

A finite-difference groundwater flow model was created using MODFLOW-2000 (Harbaugh et al., 2000) along with PMWIN Pro (Chiang, 2005) as the graphical user interface pre-processor, and post-processor. The most recently published USGS Shelter Island groundwater model, created by Schubert (1999), was used as a starting point for this model. The USGS provided the original MODFLOW files, but due to formatting differences in the raw data files, PMWIN Pro was unable to read the USGS files. However, the original MODFLOW run output file provided enough information to enable a reconstruction of the model as described in Schubert's 1999 USGS report. Ultimately, the model was run with SEAWAT-2000 in order to fully model the moving interface between saltwater and freshwater, but because the variable density function of SEAWAT is not compatible with the sensitivity and parameter estimation processes of MODFLOW-2000, it was useful to run the model first using MODFLOW-2000 in order to make use of those features (Langevin et al., 2003)

Model Geometry

The Schubert (1999) model of groundwater flow on Shelter Island consisted of a cross-sectional area 187.5-ft deep and 16,000-ft wide cutting east-west across the island (Figure 7). The model grid consisted of 25 vertical layers, each 7.5 feet thick, starting from 5 feet above mean sea level to 182.5 feet below sea level. The range was originally chosen to include the highest measured head elevation to a depth below the top of the Pleistocene marine clay layer. Within this clay layer, the groundwater flow was believed

to be negligible. The horizontal grid spacing ranged from 400 ft off shore and inland to 50 ft near the freshwater/saltwater interface. The new model created for this study used the same grid spacing as seen in Figure 9.

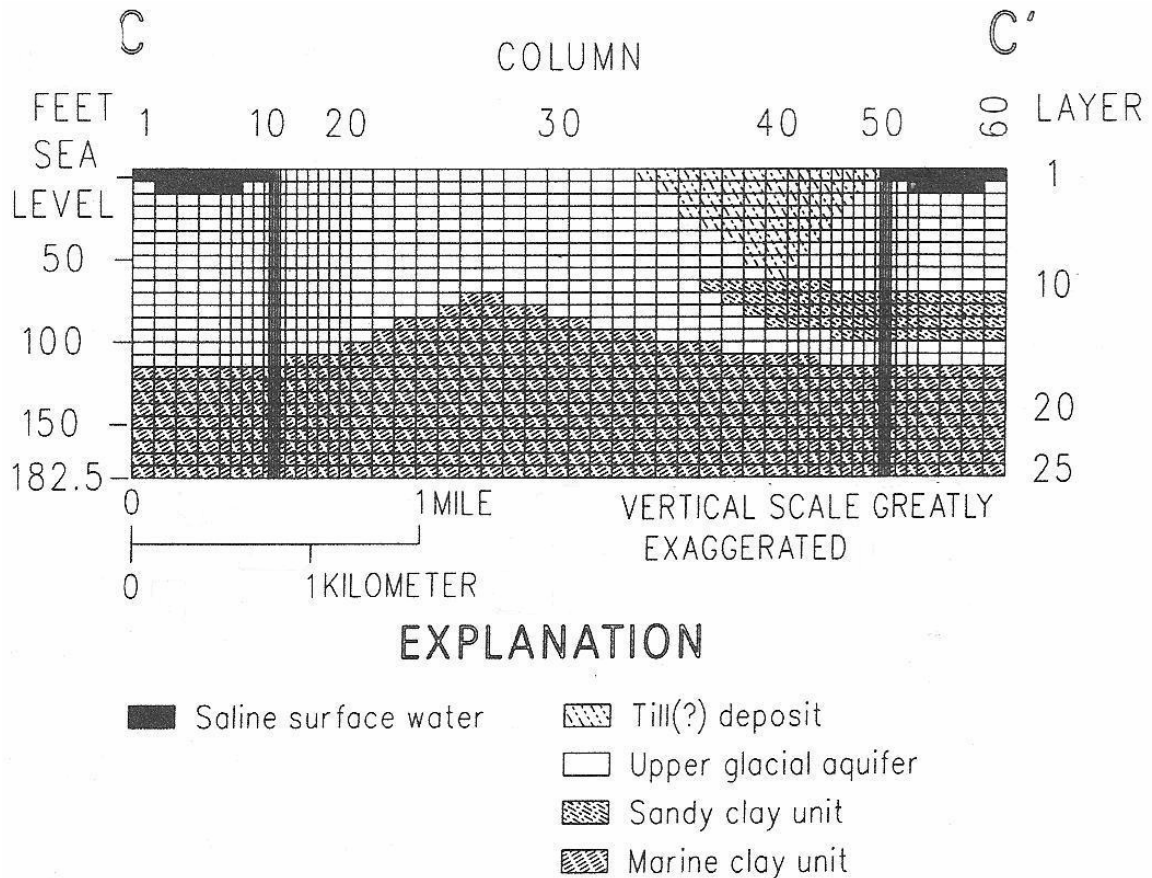


Figure 9: Grid spacing for the finite-difference model created from cross-section C-C' (modified from Schubert, 1999)

Boundary Conditions

The water table surface acts as the recharge boundary and discharge occurs near shore as submarine groundwater seepage. The freshwater/saltwater interface acts as a nearly impermeable boundary that moves under prevailing hydrologic conditions (Schubert, 1998). Thus, the model included a top layer constant-flux boundary to represent the water table and recharge, two constant head boundaries to represent shoreline underflow of freshwater to the saline surface, two constant head boundaries to

represent sub-sea discharge near the clay layer, and three no-flow boundaries that represent the freshwater/saltwater interface as shown in Figure 10.

For this study, the top model layer was defined as unconfined and the rest of the layers were allowed to be fully convertible between confined and unconfined with variable transmissivity during the simulation. The boundary conditions, as described in Figure 10, are applied to the model as seen in Figure 11. It should be noted that the sandy clay unit with the constant-head boundary E-F (Figure 10) was modeled with another lower constant-head boundary between its base and the marine clay layer that is not shown in Figure 10, but is shown in Figure 11.

For the SEAWAT-2000 model run in this study, the recharge interface and constant head boundary representing the seawater surface surrounding the island did not change. However, because SEAWAT can correctly model the freshwater/seawater interface, it was unnecessary to create a series of no-flow boundaries to represent this interface. Instead, the boundaries were removed and the edges of the freshwater lens were delineated by the concentration of salt in each cell. Thus, all the grey no-flow cells seen in Figure 12 were changed to active cells and the salt concentration for those cells was increased to that of seawater. This created the initial freshwater/saltwater interface which was then free to move during the simulation.

Additionally, for the SEAWAT-2000 model, a general head boundary condition was initially used along the sides and bottom perimeter cells. Without a general head boundary condition, the grid perimeter is interpreted as a no-flow boundary, a situation that does not describe field conditions. However, it was determined during subsequent simulations that the perimeter general head boundary was unnecessary since there was no

substantial flow across the general head boundary at the grid perimeter. The bay saltwater surrounding Shelter Island provides a constant head source or sink for any saltwater flow caused by movement of the saltwater/freshwater interface.

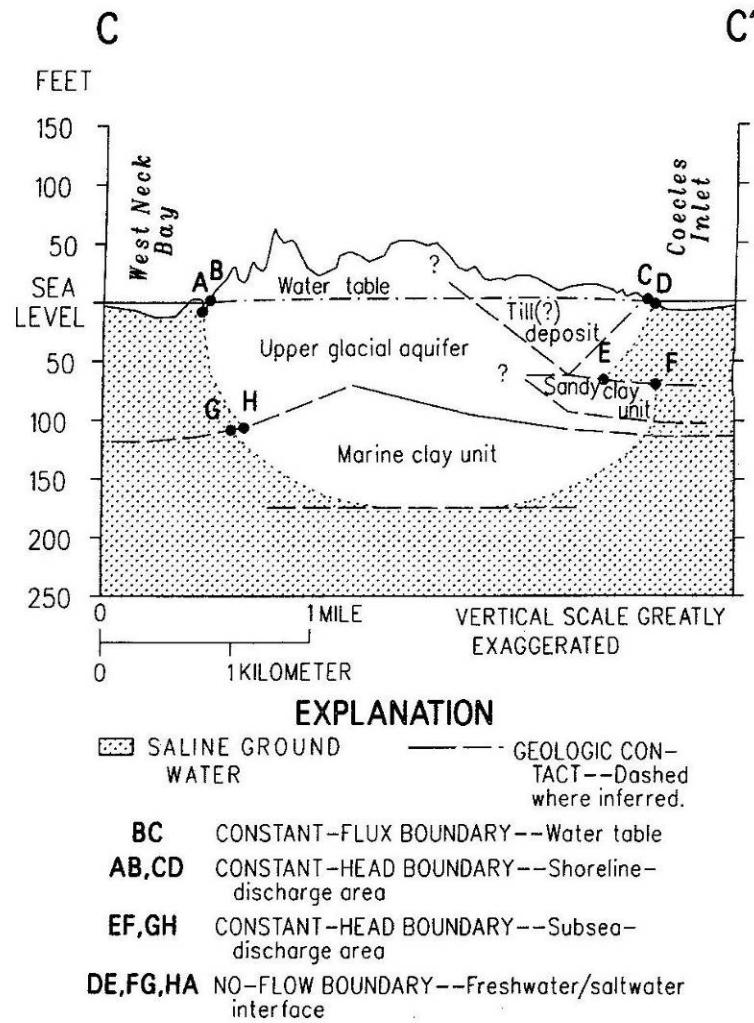


Figure 10: Model boundary conditions from Schubert (1999) study (modified from Schubert, 1999)

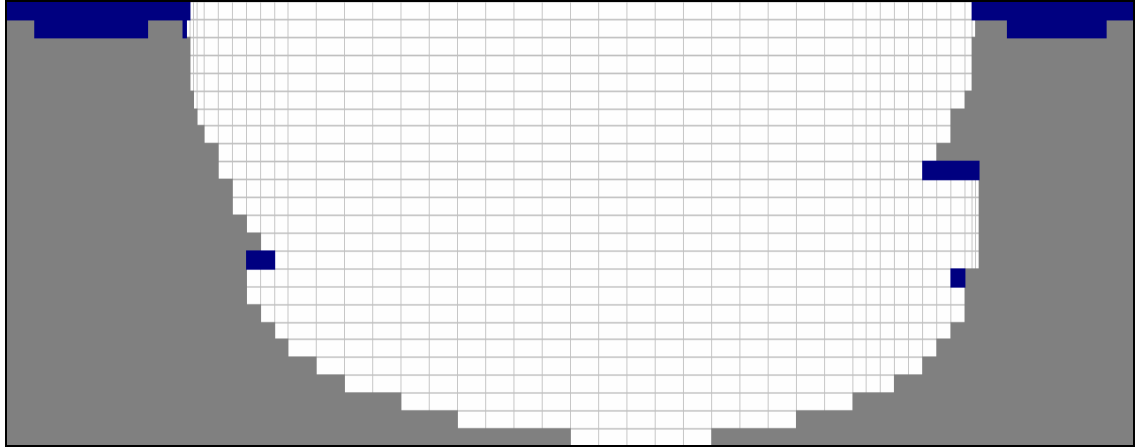


Figure 11: Boundary Conditions for initial model. Grey areas are no-flow cells. Blue cells are constant head boundaries.

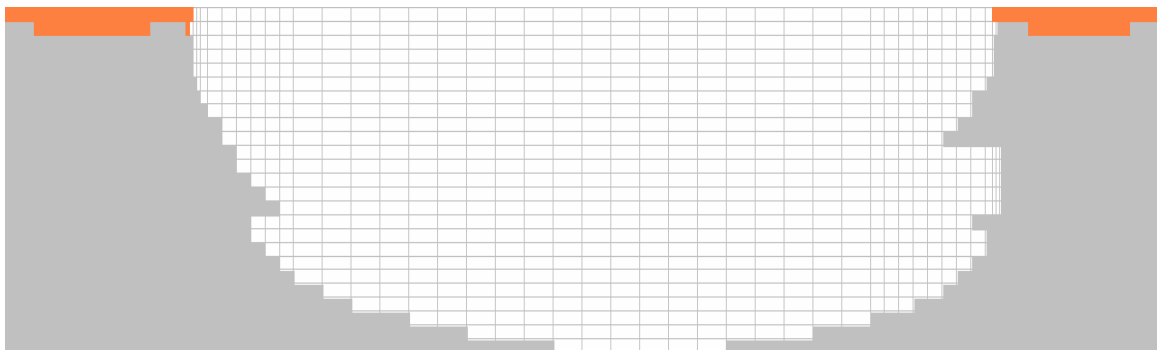


Figure 12: Boundary conditions for SEAWAT-2000 model. Orange cells represent constant head boundaries. Grey cells represent saltwater concentrations of 2.18 lbs/ft³.

As described in a subsequent section of this paper, it was determined during the course of the study that a second, simplified version of the SEAWAT-2000 model should be constructed that ignored flow to the Pleistocene marine clay layer. For this revised model, all marine clay layer cells were changed to inactive status. The resulting revised model consisted of only the top 16 layers (Figure 9) of the original model and the bottom edge of the new model was a no-flow boundary representing part of the Pleistocene marine clay layer (Figure 13).

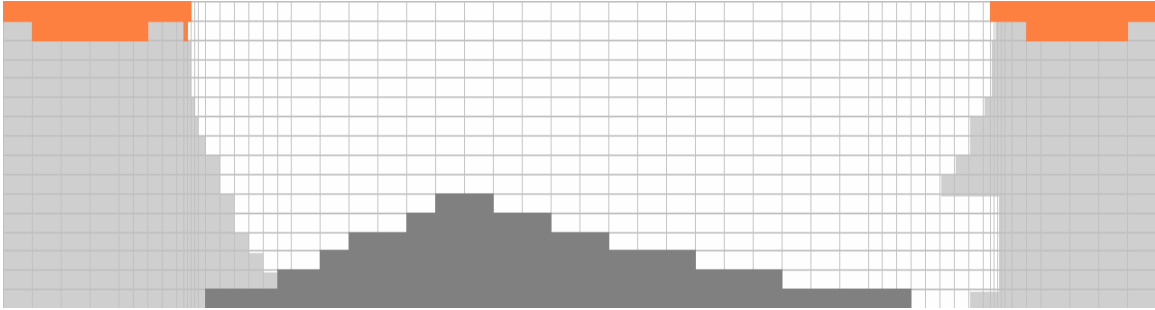


Figure 13: Boundary conditions for second SEAWAT-2000 model. Orange cells represent constant head. Light grey cells represent saltwater concentrations of 2.18 lbs/ft³. Dark grey cells represent the Pleistocene marine clay layer (inactive).

Seawater

A value of 0.4 ft was used in the Schubert (1999) model as the difference between mean sea level and the National Geodetic Vertical Datum (NGVD) of 1929 based on readings obtained from tidal measurement stations within Peconic Bay (Table 2).

Table 2: National Geodetic Vertical Datum (NGVD) and mean sea-level within Peconic Bay. All values are in feet (modified from Schubert, 1999)

Location	Mean Sea Level - NGVD	Mean High Water - NGVD	NGVD- Mean Low Water
South Jamesport	0.32	1.71	1.35
Threemile Harbor	0.48	1.70	0.98

The O'Rourke (2000) model set a constant head boundary condition at the shores of 0.5 ft to represent sea level referenced to the NGVD of 1929. In order to reproduce the Schubert conditions, 0.4 was chosen as the mean sea level for the initial run of the model in this study.

In the MODFLOW-2000 version of the Shelter Island model, freshwater equivalent heads were used where freshwater/saltwater interfaces existed, such as boundaries E-F and G-H in Figure 10 using:

$$h_{fe} = \frac{z}{40} + h_{msl} \quad (11)$$

where h_{fe} is the freshwater equivalent head and h_{msl} is the mean sea level (Schubert, 1999). However, in the SEAWAT-2000 version of the Shelter Island model, the freshwater/saltwater interface was denoted by the concentration differences of salt in freshwater, approximately 0 lbs/ft³, and seawater, 2.18 lbs/ft³ (Masterson, 2004).

Recharge

Shelter Island has an area of 7,670 acres or approximately 12 square miles (Schubert, 1998). Because there are no significant streams on Shelter Island, precipitation that is not lost to evapotranspiration becomes recharge to the aquifer (Soren, 1978). Miller and Frederick (1969) determined that the mean annual precipitation for Long Island was between 43 and 45 inches. For the years 1974 to 1983, Simmons (1986) computed a rate of precipitation of 47 inches/yr. According to Nemickas and Koszalka (1982), the rate of evapotranspiration on Long Island is 50%, and the rate of overland runoff is 1%. Peterson (1987) also used a recharge rate of 50% as a good approximation. However, Steenhuis et al. (1985) suggested an alternative method using a recharge rate between 75% and 90% from October 15 to May 15 and a recharge rate of 0% for the warmer summer months when evapotranspiration equals or exceeds precipitation. See Appendix I for an application of these recharge rates to the precipitation measured at the weather stations surrounding Shelter Island. Because long-term steady-state conditions were of primary concern in this study, the 50% recharge rate approximation was used for all modeling.

Geologic Parameters

Soren (1978) determined that Shelter Island sand has a horizontal hydraulic conductivity between 200 and 270 ft/day and a hydraulic gradient of 0.00115. According to Smolensky et al. (1989), Long Island sand has a horizontal hydraulic conductivity of 270 ft/day with an anisotropy ratio of 10:1. The Pleistocene Smithtown Clay on central Long Island has a vertical hydraulic conductivity of 0.035 to 0.07 ft/day (Misut and Feldman, 1996). Porosity is estimated to be an average of 30% (Franke and McClymonds, 1972; Soren, 1978). A study of the North Fork of Long Island by Schubert et al. (2004) used a horizontal hydraulic conductivity of 200 ft/day for upper glacial outwash, a horizontal hydraulic conductivity of 80 ft/day for upper glacial moraine, an anisotropy ratio of 10:1, and a vertical hydraulic conductivity for confining units of 0.4 ft/day.

The O'Rourke (2000) model used hydrogeologic parameters as described in Table 3. For transient model runs, specific storage was set at $1 \times 10^{-6} \text{ ft}^{-1}$ and specific yield was set to 0.25.

Table 3: Defined geologic units and parameters used in O'Rourke(2000) model.

Sediment Type	Horizontal Conductivity (ft/day)	Vertical Conductivity (ft/day)	Porosity
Fine Sand	232	2.32	0.30
Medium Sand	232	23.2	0.30
Coarse Sand	300	30	0.25
Silt and Clay (till)	5	.5	0.40
Clay	1	0.05	0.45

Four hydrogeologic units are represented in this study's model as shown in Figure 9: (1) a poorly sorted mixture of clay, silt, sand, and gravel referred to as till, (2) upper

glacial aquifer moraine and outwash, (3) a sand clay unit, and (4) the Pleistocene marine clay unit (Schubert, 1999). The parameters used in the original Schubert (1999) model after calibration are shown in Table 4.

Table 4: Defined geologic units and parameters used in Schubert (1999) model. Conductivities varied slightly at borders between hydrogeologic units.

Layer	Horizontal Conductivity (ft/day)	Vertical Conductivity (ft/day)
Till	30	0.30
Moraine and outwash	320	32
Sandy clay	10	0.10
Pleistocene marine clay	4	0.002
Porosity (all layers)	30%	

Pumping

In 1983, by which time population had stabilized according to the 2000 US Census, Shelter Island had three local water supply facilities serving 25% of the population. It was estimated that the total annual pumpage for the island was 262 million gallons (Simmons, 1986) or approximately 96,000 ft³/day.

According to Franke and McClymonds (1972), about 85% of public water pumpage is returned to groundwater in non-sewered sections of Long Island. Only a small portion of Shelter Island is sewerred and most water returns through septic systems relatively close to where it was pumped (Schubert, 1998). Assuming an 85% return rate, only 14,400 ft³/day is lost to pumping. Likewise, agricultural withdrawal, the only appreciable non-residential water use on Shelter Island, is estimated at 4,600 ft³/day (Schubert, 1998). Together these pumping rates are less than 1% of the estimated 1.72 million ft³/day of submarine groundwater discharge for the island. Thus, pumping is ignored in this study.

Other Assumptions

Because the vertical cross-section chosen for Shelter Island is not perpendicular to all potentiometric contours (Figure 7), the model does not strictly represent two-dimensional flow. However, the cross-section was chosen such that most water-table contours, especially near-shore, are perpendicular to the model and will provide reasonably good results (Schubert, 1999).

Also, the study did not take land subsidence from dewatering into account as recommended by Titus and Narayan (1996). Because the water table on Shelter Island is close to sea level, excessive freshwater pumping would create negligible amounts of dewatered land subsidence (Davis, 1987). Additionally, since pumping is ignored in this study, it is reasonable to also ignore subsidence caused by pumping.

Because regional tectonic subsidence rates were not taken into account in this study, over the maximum timeframe of this study, the relative sea level rise is underestimated. According to glacial isostatic adjustment theory, since the last glacial maximum 21,000 years ago, the crust formerly depressed under the North American ice sheet has been visco-elastically rebounding. Concurrently, a crustal bulge at the glacial edge has been subsiding (Peltier, 1999). Because Long Island exists in the area of proglacial forebulge collapse, the area has a rate of sea level rise in excess of eustatic sea level rise. Subtracting an average absolute sea level rise rate for the eastern North American coast of 1.3 mm/year (Gornitz, 2000) from the relative sea level rise for Montauk, NY and Port Jefferson, NY of 2.27 and 2.20 mm/year respectively (Gornitz et al., 2002), yields a regional subsidence rate of 0.90 to 0.97 mm/year. Over the course of a century, this translates to 90 to 97 mm (3.5 to 3.8 inches) of subsidence. Since Shelter

Island is between Port Jefferson and Montauk, assuming a constant subsidence rate in the future, by the end of the study, the local sea level should be an additional 3.5 to 3.8 inches higher than the eustatic averages given in the IPCC.

Calibration

In the Schubert (1999) model, hydraulic conductivity parameters, freshwater/saltwater interface position, and precipitation data were all adjusted by trial and error until reasonable matches with field monitoring well measurements were obtained. Calibration was performed for March 1995 during which water levels were approximately 24% below long-term averages due to low recharge in 1994 that was 26% below average. Therefore, the model was calibrated using March 1995 well head levels and a recharge of 50% of 1994 precipitation resulting in recharge of 0.00377 ft/day per unit area which was arrived at from the 1994 Greenport annual rainfall datum listed in Appendix I as follows:

$$\frac{33.07" \text{ rain}}{\text{yr}} \times \frac{1 \text{ yr}}{365.25 \text{ days}} \times \frac{1 \text{ ft}}{12"} \times 50\% = 0.00377 \text{ ft/day} \quad (12)$$

During two model runs, O'Rourke (2000) used the following recharge estimates: 0.009823 ft/day for a steady-state calibration March 1999 run, and 0.01081 ft/day for a steady-state March 1994 validation run.

In the Schubert (1999) study, the freshwater/saltwater interface, modeled as a no-flow boundary, was placed according to field measurements and calculations using the modified Ghyban-Herzberg formula (equation 11). The resulting model head simulations were compared to field observation in Table 5. The largest differences between the simulated and measured water levels were found near the center of the island and were

likely due to the most substantial deviation from two-dimensional flow at that location (Figure 7). Discrepancies near the shoreline were attributed to the effect of the tide on near shore monitoring wells which was ignored in the Schubert model.

Table 5: Measured and simulated water levels measured in feet above National Geodetic Vertical Datum of 1929 for Schubert (1999) model. (modified from Schubert, 1999)

Well Number	Model Cell		March 1995 Water Level			Simulated long-term water level
	Column	Layer	Measured	Simulated	Difference	
106168	14	7	1.92	1.18	0.74	1.44
51172	18	3	2.02	2.04	-0.02	2.59
106206	19	2	2.33	2.19	0.14	2.78
106169	19	11	2.34	2.19	0.15	2.79
106171	26	4	2.96	3.68	-0.72	4.75
106170	26	8	2.97	3.67	-0.70	4.75
106173	34	5	3.40	4.44	-1.04	5.75
106172	34	15	3.27	4.30	-1.03	5.54
51179	40	7	3.56	3.49	0.07	4.46
106174	40	14	3.38	3.50	-0.12	4.42
106175	48	2	1.50	1.10	0.40	1.31

In the O'Rourke (2000) model, the standard deviation between observed and simulated monitoring well heads was 0.342 ft for the steady state calibration and 0.327 ft for the transient calibration. Validation run standard deviations were 0.424 ft and 0.395 ft for the steady state and transient runs respectively. Due to tidal influences, near shore wells were not used during the calibration process.

The initial run of the model in this study, replicating the Schubert (1999) study, was run steady-state. Initial head conditions were set at 5 ft. for all cells except constant-head boundaries, as shown in Table 6, which were calculated using Equation (11).

Table 6: Initial Head Conditions for first model run

Constant-Head Boundary (Figure 10)	Initial Head (ft)
A-B, C-D	0.4
E-F	2.05
G-H	3
I-J	3.2

After the original Schubert (1999) data was duplicated, the model was recalibrated using two automated parameter estimation programs: PEST, which uses the Gauss-Marquardt-Levenberg method (Doherty, 1994), and UCODE, which uses the Gauss-Newton iterative method to find the weighted least squares objective function (Hill, 1998).

In order to use either PEST or UCODE, the parameters to be estimated were first selected and defined. For this model, either program had the capability to estimate the horizontal and vertical hydraulic conductivity and recharge. The grid spacing, boundary conditions, initial head values, and porosity were not adjusted in any of the parameter estimation runs. An initial parameter estimation run was restricted to hydraulic conductivity. This was accomplished by defining eight different hydraulic conductivity regions, four vertical and four horizontal, within the model corresponding to the various hydrogeological units. Next, the head observations listed in Table 5 were entered into PEST and the program was run in the parameter estimation mode.

Parameter estimation using PEST proved unsuccessful. The inverse modeling returned parameters outside of reasonably expected results. Even when restricted to estimating only the horizontal hydraulic conductivities of the four geological units, PEST did not give acceptable results. Specifically, the horizontal conductivity of the clay layer, determined by Schubert to be 4 ft/day was estimated by PEST to be 400 ft/day, the upper bound set within PEST for that parameter. Hill (1998) recommends rejecting inverse modeling results that are obtained by an imposed upper or lower parameter limit because it suggests potential inverse model instability. In those cases, it is recommended that prior information be used to estimate the most probable parameter value. In this case, the

prior information of the Schubert model results and previously mentioned published literature provided the best estimates. Thus, automated parameter estimation was abandoned.

A head value scatter diagram was created (Figure 14) to compare the model and observed values when PEST parameters were substituted into the model. Despite the unlikely parameter values estimated by PEST, the variance of the scatter diagram was 0.15 compared to a variance of 0.47 for the original Schubert parameters. The same process was repeated with UCODE, with similarly unsuccessful results. A resulting head value scatter diagram for the UCODE parameters had a variance of 0.58, worse than those generated by the original parameters.

Calibration of the SEAWAT-2000 model presented its own unique problems. Because SEAWAT is not compatible with PEST (Langevin et al., 2003), all calibrations were performed by trial and error while working within the limits of parameter values previously described. Additionally, although SEAWAT-2000 can be run with the flow portion of the model in a steady state condition, the solute transport portion of the model, controlled by MT3DMS-derived code, must run as a transient model. Since the flow patterns may be affected by any appreciable redistribution of salt within an aquifer, it is recommended that both portions of the model be run in transient mode (Guo and Langevin, 2002).

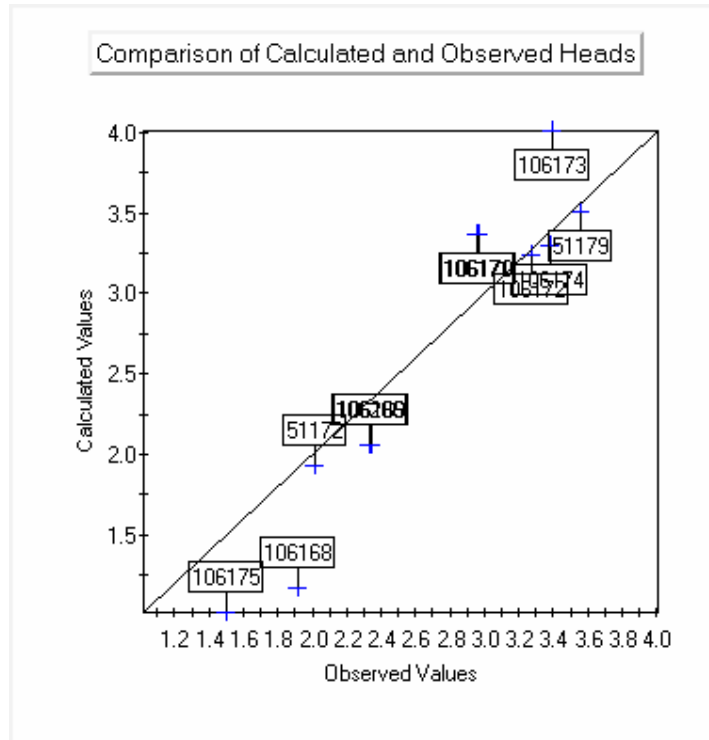


Figure 14: Head value scatter diagram from PEST forward run. The variance is 0.15. The standard deviation is 0.39 ft.

In order to run the model in transient mode, a specific storage and specific yield were required. Based on the O'Rourke (2000) model and recommended specific storage (Domenico, 1972) and recommended specific yield values (Domenico and Schwartz, 1998), a specific storage of $1 \times 10^{-4} \text{ ft}^{-1}$ and a specific yield of 0.25 were chosen.

As with any transient model where initial conditions are run to a steady-state condition, it was necessary to determine how long to run the model. Because the original Schubert (1999) model found that the longest particle travel time was about 1,800 years, the SEAWAT-2000 model was run for 700,000 days (approximately 1,926 yrs). As seen in Figure 15, the model becomes steady-state at approximately 350,000 days (almost 1000 years). At the end of the transient model run, the variance of the head scatter diagram was 0.49.

However, the concentrations and head contour diagrams showed a failure of the model to correctly model the freshwater/saltwater interface within the marine clay layer. According to the Schubert (1999) model, almost all flow occurred in the upper glacial aquifer. Therefore, a model that excluded the flow within the marine clay unit still approximates the aquifer conditions. The second version of the SEAWAT-2000 model that was created to model only the upper glacial flow (see Figure 13), reached steady-state far faster than the original model. Figure 16 shows that the second model reaches equilibrium within 10,000 days (approximately 27 years). Thus, for all subsequent model runs, each simulation was run for 20,000 days in order to ensure that the transient model had run to full steady-state conditions.

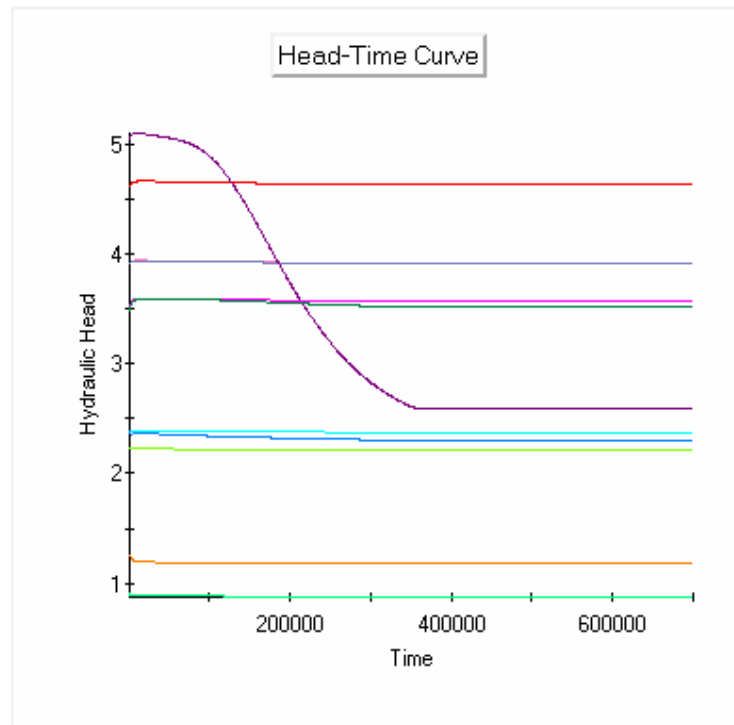


Figure 15: Head-Time curve for the initial SEAWAT-2000 model showing head levels reach steady state in 350,000 days. Vertical axis units are feet and horizontal units are days.

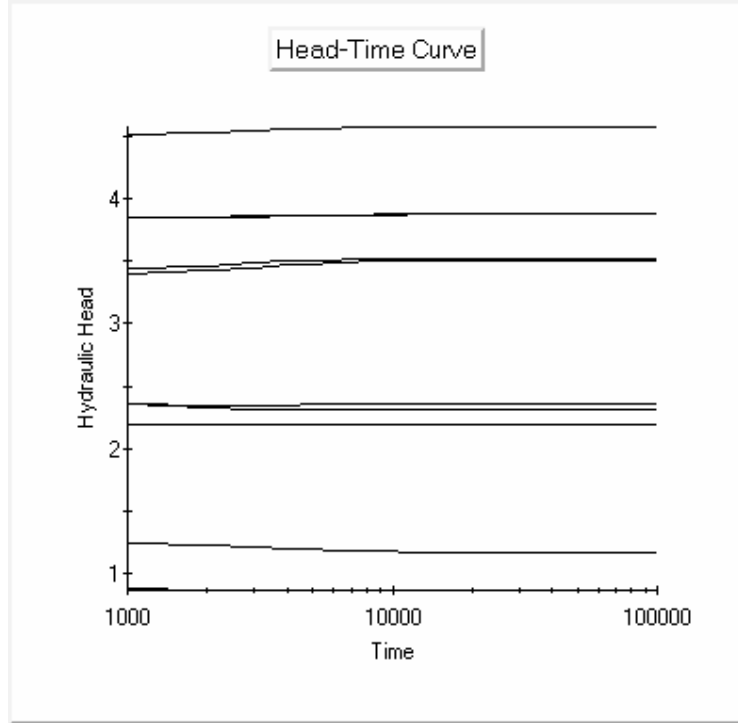


Figure 16: Head-Time curve for the revised SEAWAT-2000 model showing head levels reach steady state in 10,000 days. Vertical axis units are feet and horizontal units are days.

Using the revised SEAWAT-2000 model, a calibration was performed using trial and error methods. Ultimately, a variance of 0.38, marginally better than the original Schubert (1999) model variance of 0.47, was achieved using the values in Table 7. All subsequent modeling used those hydrogeologic parameters.

Table 7: Parameters used for each geologic unit in revised SEAWAT-2000 model. Conductivities varied slightly at borders between hydrogeologic units.

Layer	Horizontal Conductivity (ft/day)	Vertical Conductivity (ft/day)
Till	60	0.60
Moraine and outwash	320	32
Sandy clay	40	0.40
Pleistocene marine clay	inactive	inactive
Porosity (all layers)	30%	

Sensitivity Analysis

A sensitivity analysis was performed on the MODFLOW version of the model in this study using PEST. For the four horizontal hydraulic conductivities estimated in the initial calibration run, the relative sensitivities are described in Table 8. The model output is two orders of magnitude more sensitive to the assigned hydraulic conductivity values for the till and moraine layers than the clay layers. Thus, the relative insensitivity of the clay layers makes inverse modeling of those parameters particularly difficult.

Table 8: PEST Parameter Sensitivity Analysis

Parameter (Unit)	Horizontal K (ft/day)	Relative Sensitivity
1 (Till)	30	0.252065
2 (Sandy clay)	10	1.868586E-02
3 (Pleistocene marine clay)	4	2.934729E-02
4 (Moraine and outwash)	320	3.32075

A sensitivity analysis of the observation data (see Table 9) shows a negligible preference for the data collected towards the center of the island. Thus, if further data were collected, there is no strong preference for any location along the island cross-section.

Table 9: PEST Observation Sensitivity Analysis

Well Number	Model Cell		Sensitivity
	Column	Layer	
106168	14	7	0.3081780
51172	18	3	0.7306555
106206	19	2	0.7992607
106169	19	11	0.7982863
106171	26	4	1.486451
106170	26	8	1.486451
106173	34	5	1.693937
106172	34	15	1.431302
51179	40	7	1.102480
106174	40	14	0.9957142
106175	48	2	0.2832927

Because variable-density modeling is more sensitive to grid spacing than constant-density models (Guo and Langevin, 2002), the Shelter Island model was refined to a uniform horizontal grid spacing of 50 ft in order to test if the grid spacing caused numerical instability. The vertical spacing was left at 7.5 ft (Figure 17). The results of a simulation run were nearly identical to simulations run with the original grid spacing, but a slight improvement in variance to 0.34 occurred in the head scatter diagram. Given the similarity of results and the considerable increase in model run time, the original grid spacing was used for all remaining simulations.

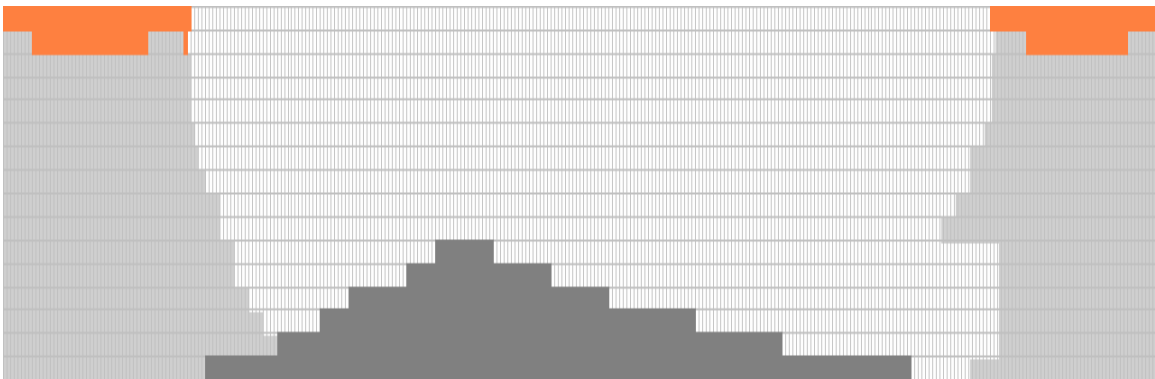


Figure 17: Uniform horizontal grid spacing of 50 ft used in grid sensitivity analysis.

Validation

In order to perform a validation of the calibrated model, additional well head data for history matching was obtained from the Suffolk County Department of Health. The SCDH has data for Shelter Island from 1974 to the present and two of the wells they regularly monitor were used in the original Schubert (1999) study: Well 51172 and Well 51179. Looking through the well head data and precipitation readings (see Appendix I), it was apparent that years 1994 and 1995, when the model was calibrated, were below the 44-inch, long-term average precipitation. However, 1996 was an above average year with a total precipitation of 56.39 inches. Two dry years followed by a wet year provided

a relatively simple test of whether the model would correctly respond to a substantial perturbation of recharge. So a simulation was run with the previous calibration results as the initial conditions followed by two stress periods; 1995 (another dry year) and 1996 (a higher recharge year). The 1996 results were then compared to the two well head observations from March of 1997 in order to consistently use readings from the same time of year and with a one year delay. The results are shown in Table 10. Given that the well head data provided by SCDH shows considerable variation throughout any single year, the variance of 0.45 was reasonable and the validation was acceptable for this study.

Table 10: Comparison of the calibration and validation process results. Precipitation data comes from the Greenport station (see Appendix I). Well head data were taken from March of the following year for modeling consistency.

	Calibration	Validation
Year	1994	1996
Precipitation (inches)	33.09	56.39
Recharge rate (inches/day)	0.00377	0.00643
Year	1995	1997
Well 51172 (ft) Observed	2.02	3.28
Well 51172 (ft) Calculated	2.18	2.63
Well 51179 (ft) Observed	3.56	5.27
Well 51179 (ft) Calculated	3.42	4.58

Results

The initial run of the reconstructed Schubert (1999) model shown in Figure 18 agreed with the results of the original model. In a cell-by-cell comparison to the original Schubert (1999) model, the reconstructed model had an average head difference of -0.03 ft and a standard deviation of 0.1 ft. These small head differences were most likely attributed to each model being run with a different version of MODFLOW with different numerical solution packages. Since the two models were essentially equivalent, it was decided to move to the next step of integrating variable density flow modeling using SEAWAT.

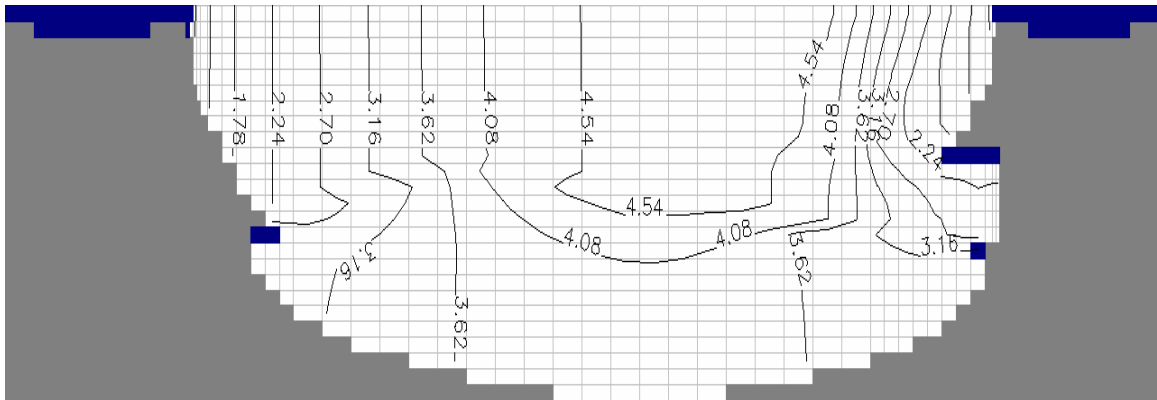
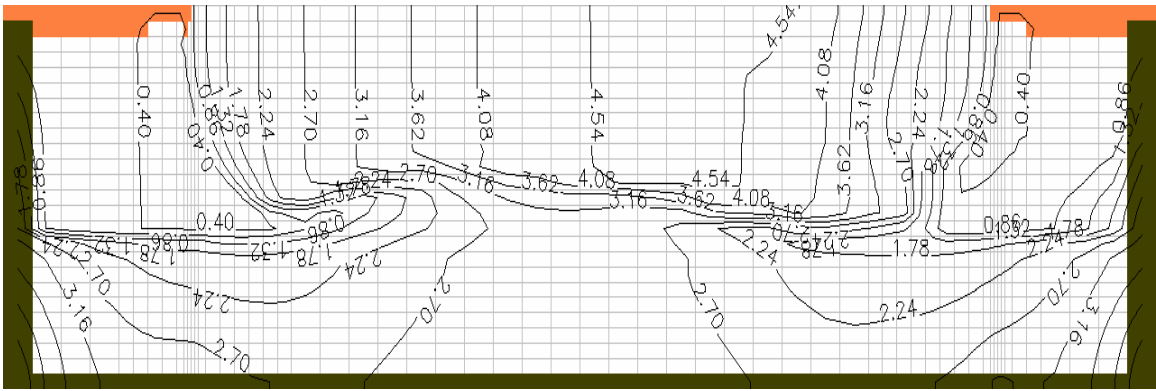


Figure 18: Reconstructed Schubert model run using PMWIN. Contours show head levels in feet.

The results of the first SEAWAT-2000 model are shown in Figure 19 and Figure 20 which display the hydraulic head contours and freshwater/saltwater interface, respectively. The head contours and salt concentrations along the marine clay layer interface with the upper glacial aquifer show a possible convergence issue in the model (discussed later in the paper). Because this model did not appropriately simulate the field conditions, a simplified model that ignored the minor contribution of the marine clay layer to the overall flow was created. The hydraulic head levels of the revised model are

shown in Figure 21, the saltwater/freshwater interface in Figure 22, the velocity vector field in Figure 23, and the simulated flow path lines in Figure 24.



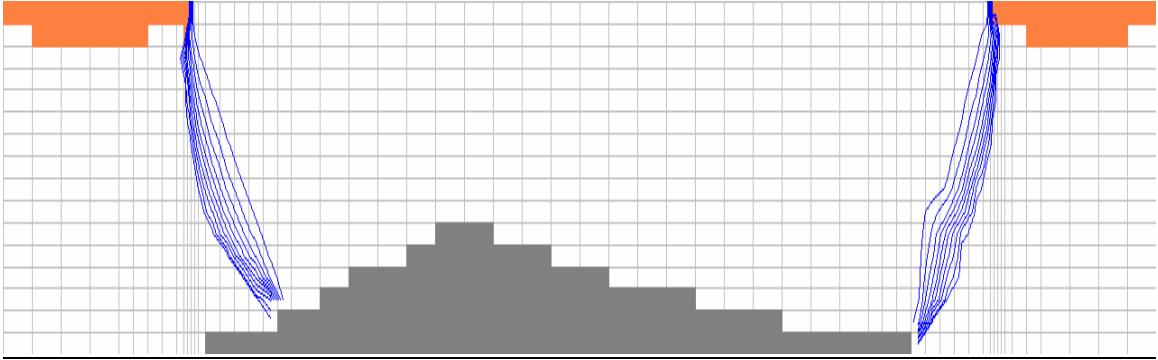


Figure 22: Revised SEAWAT-2000 model where the marine clay unit is treated as a no-flow boundary. Contours show salt concentration in 10% increments from freshwater to seawater.

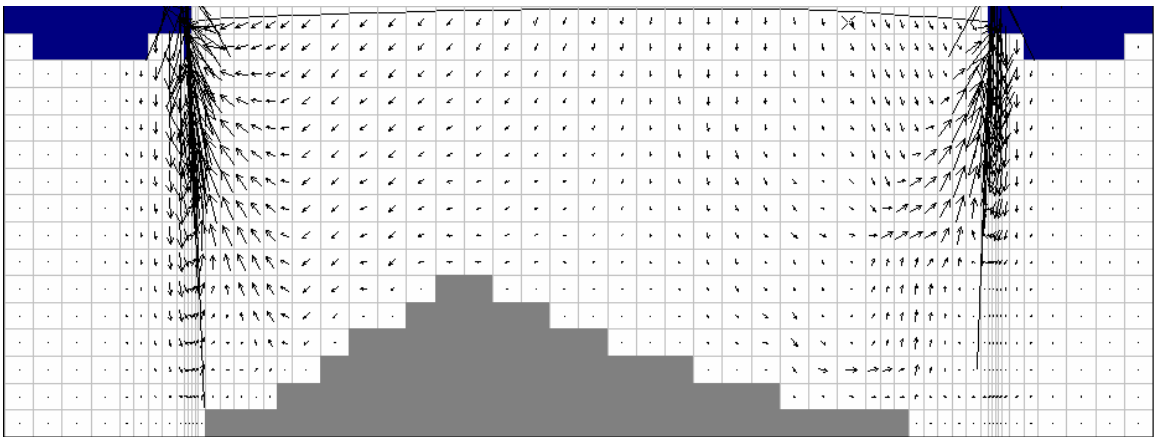


Figure 23: Relative velocity vector field for revised SEAWAT-2000 model. The arrow size in each cell is proportional to the flow velocity and points in the direction of flow.

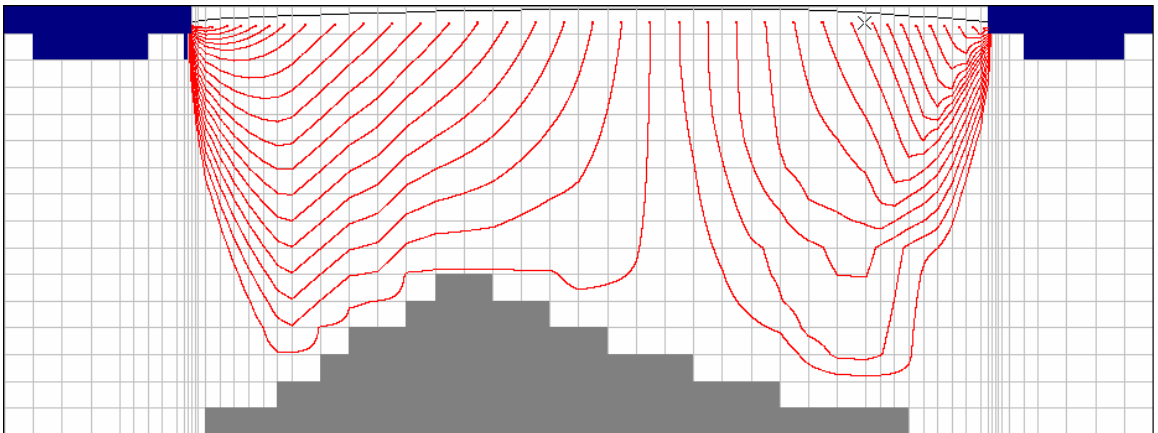


Figure 24: Flow path lines for revised SEAWAT-2000 model.

Once the model was calibrated and validated, as discussed in previous sections, the various future climate change scenarios were simulated. Three different models, as described below, were created for comparative purposes. The IPCC sea level rise predictions to the year 2099 range from 0.18 m (0.59 ft) to 0.59 m (1.94 ft) for all future human activity scenarios (Meehl et al., 2007). The effective precipitation predictions over the same time period range from -2% to 15% for the median, most likely human activity scenario in eastern North American (Christensen et al., 2007). Actual precipitation is expected to be higher but is offset by an increase in evaporation caused by higher temperatures.

Scenario 1:

Because the previous model calibration work used recharge from a below average precipitation year, a current baseline run was conducted using a long-term average annual precipitation of 44 inches (Miller and Frederick, 1969) which yields a recharge rate of 0.00502 ft/day according to Equation (12). All other parameters were unchanged.

Scenario 2:

The second simulation represented a scenario where the effects of climate change are mild with respect to groundwater resources; precipitation has increased 15% and sea levels have risen 0.6 ft. This represents the maximum predicted increase in precipitation coupled with the minimum predicted sea level rise of the 2007 IPCC report. For this simulation, the constant head cells around the island were increased from 0.4 ft to 1.0 ft and the recharge rate was increased from 0.00502 ft/day to 0.00577 ft/day. All other parameters were unchanged.

Scenario 3:

The third simulation represented a scenario where the effects of climate change are severe with respect to groundwater resources; precipitation has decreased 2% and sea levels have risen 2 ft. This represents the maximum predicted decrease in effective precipitation coupled with the maximum predicted sea level rise of the 2007 IPCC report. For this simulation, the constant head cells around the island were increased from 0.4 ft to 2.4 ft and the recharge rate was decreased from 0.00502 ft/day to 0.00492 ft/day. All other parameters were unchanged.

The results of the three simulations for the West Neck Bay side of the model are shown in Figure 25. The freshwater/saltwater interface for Figure 25 was defined as the U.S. National Secondary Drinking Water Standards suggested maximum chloride concentration of 250 mg/L (0.0156 lb/ft³) (NSDWS, 2002). Compared to the current long-term average freshwater/saltwater interface position, the Scenario 2 created an interface that moved further seaward by an average of 76 ft and a maximum of 199 ft near the bottom of the interface. Conversely, Scenario 3 created an interface that moved landward by an average of 53 ft and a maximum of 121 ft. The interface at the east end of the model showed similar results. Movement of the interface was measured as a horizontal shift and not displacement perpendicular to the interface. All horizontal distances were measured relative to the original shoreline.

The head levels for scenario 2 were higher than the current long-term average and the water table rose by an average of 0.89 feet and maximum of 1.13 ft. The head levels for scenario 3 were higher than the current long-term average and the water table rose by an average of 1.94 feet and maximum of 2.02 ft.

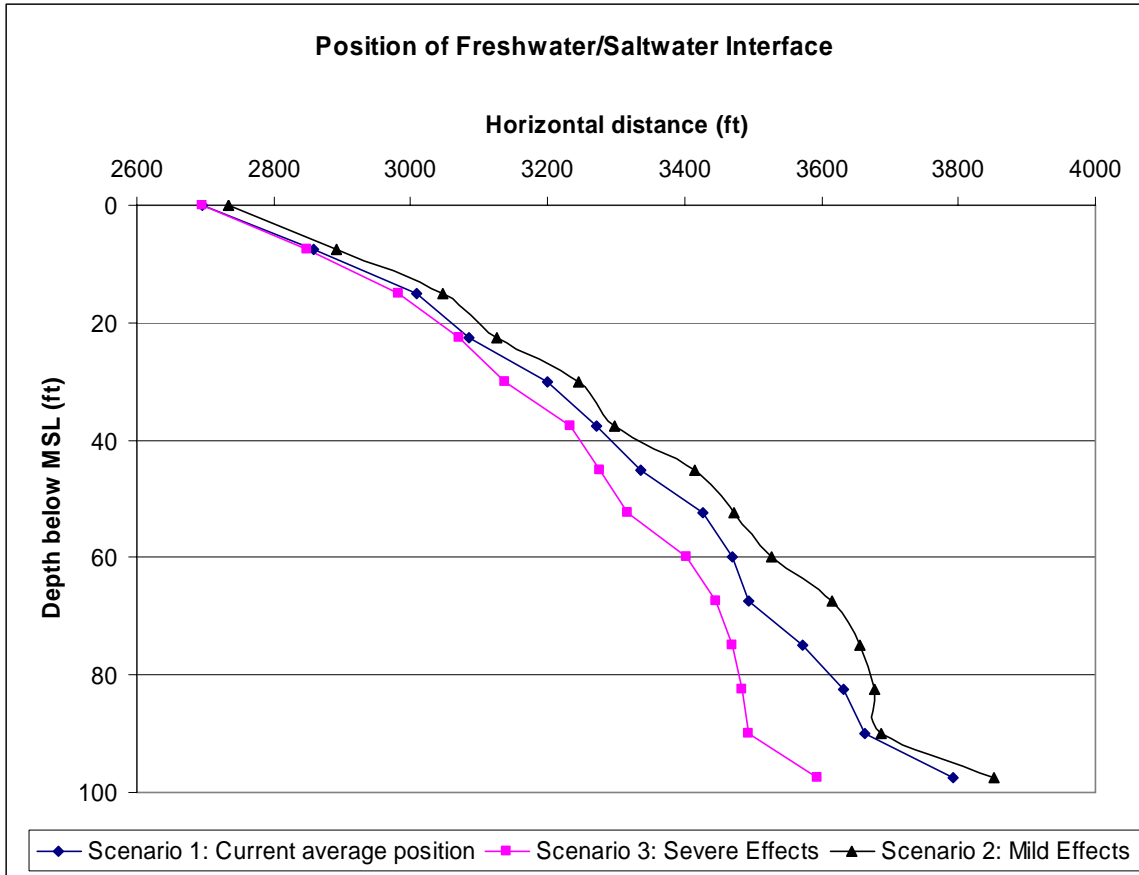


Figure 25: Position of the Freshwater/Saltwater interface in West Neck Bay for three climate change scenarios. All distances are in feet. The interface is defined as an isochlor of 250 mg/L (0.0156 lb/ft³). MSL is the mean sea-level for 2007. The horizontal position of the shoreline is assumed to be stationary in all scenarios.

The zone of diffusion of the West Neck Bay freshwater/saltwater interface for each scenario is displayed in Figure 26. Within the zone of diffusion, the concentration of salt ranges from 0 to 2.18 lbs/ft³. For simplicity, in Figure 26, the range of 0.3 to 2.1 is detailed and shows that the zone of diffusion, which has an average thickness of approximately 200 ft, becomes slightly wider under Scenario 3, where the effects of global warming are severe. However, the zone of diffusion primarily shifts with changes in sea level and recharge without appreciable overall variation in thickness.

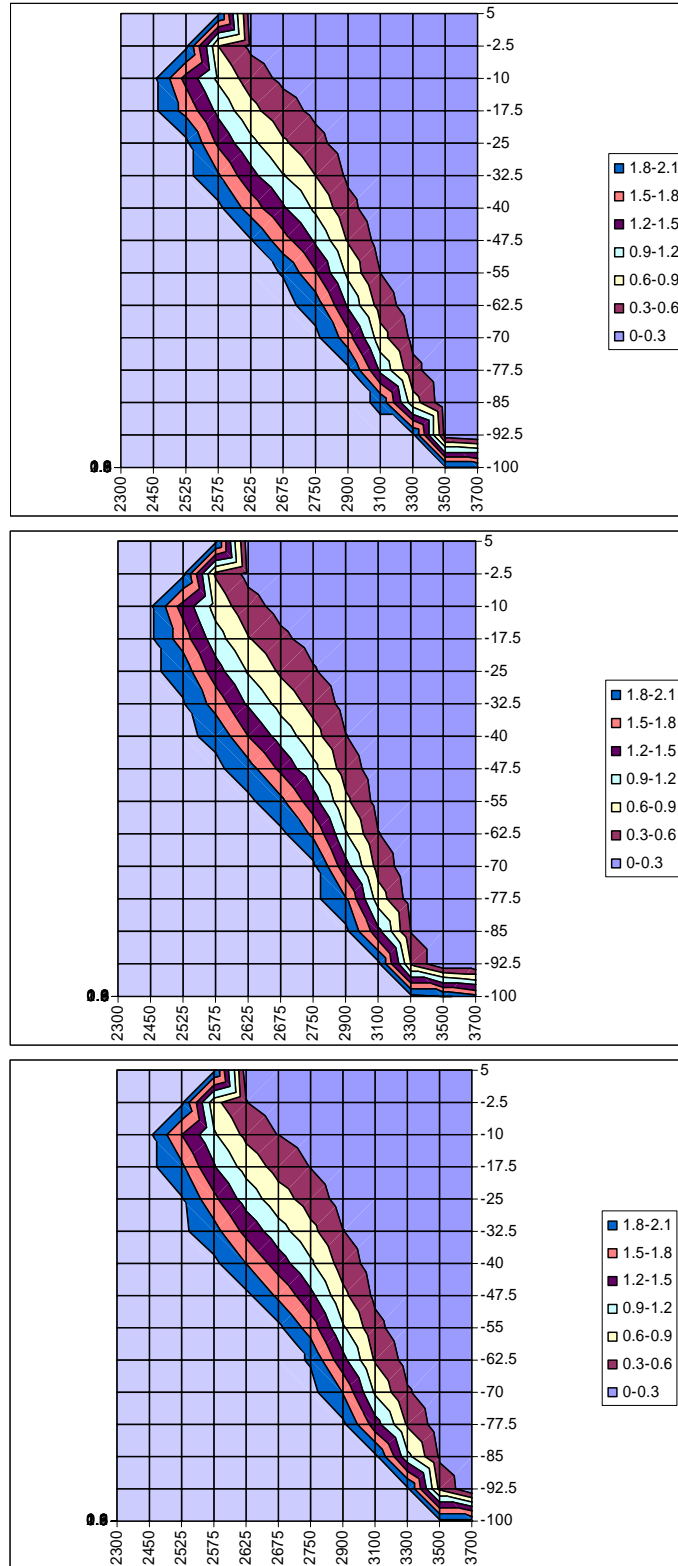


Figure 26: Zone of diffusion for freshwater/saltwater interface for Scenario 1 (top), Scenario 2 (middle), and Scenario 3 (bottom). Axes are in feet and color coded salt concentrations are in lbs /cubic ft. Note that the horizontal axis is not linear.

Discussion

The SEAWAT modeling was problematic because PMWIN is not directly compatible with SEAWAT or SEAWAT-2000. However, because PMWIN is compatible with MODFLOW-2000 and MT3DMS, it was possible to use SEAWAT-2000 with PMWIN. The user need only separately create the MODFLOW-2000 and MT3DMS input files using PMWIN as the pre-processor and then combine them to run SEAWAT-2000. The SEAWAT-2000 documentation (Langevin et al., 2003) explains how to create the additional files that allows SEAWAT-2000 to read and write to the MODFLOW-2000 and MT3DMS files. Additionally, the extra data files, created with a text editor, define the reference densities of the variable density fluid models. When the simulation is complete, PMWIN can be used as the post-processor without additional file manipulation.

The original SEAWAT-2000 model attempt appeared to have convergence problems with regards to the Pleistocene marine clay unit. Guo and Langevin (2002) outline several issues that cause problems with variable density flow models. With respect to the finite difference grid, the need for cell volume uniformity and higher resolution, particularly vertical resolution, are potential issues for constant-density simulations that are converted to variable-density. In the case of the Schubert (1999) model, the relatively small and uniform vertical resolution may have prevented some numerical instability issues. Furthermore, using a higher resolution and uniform horizontal grid spacing in the sensitivity analysis did not reveal any stability issues related to grid size. However, an even finer vertical and horizontal grid spacing may allow for an appropriate solution.

Other model design problems that can give rise to numerical instability include: initial conditions that are very far from equilibrium, rapidly changing boundary conditions, and large differences in hydrogeologic unit properties in adjacent cells. Because the initial head conditions and general head boundary values were based on the previous Schubert (1999) model, they are an unlikely source of instability. The large change in hydraulic conductivities, a ratio of almost 100:1, between the upper glacial sand unit and the marine clay unit interface, are a more likely cause of numerical instability. Adding an intermediate layer to minimize the sharply differentiated units might solve the model instability. However, it is important not to stray too far from the actual known geologic conditions of the site merely to work around the mathematical weaknesses of any particular modeling approach. In this case, excluding the contribution of the marine clay layer from the simulation was deemed to be the best compromise.

The slow response time of the marine clay unit is an additional reason for excluding it from the model. According to the particle-tracking performed by Schubert (1999), the average travel time through the marine clay unit was 1,800 years. Travel time for the upper glacial unit flow averaged about 20 years with almost all flow less than 50 years. The freshwater/saltwater interface in the upper glacial aquifer responds within decades to changes in recharge and sea level, while the interface within the marine clay unit responds over millennia. Because the simulation time of this study is less than a century, it is reasonable to treat the marine clay unit as impermeable and a no-flow boundary within that timeframe. Additionally, rapid climate change, as predicted by the IPCC, should cause a distorted freshwater/saltwater interface that could be difficult to model due to possible discontinuities near the interface of the two hydrogeologic units. It

is also possible that the current freshwater/saltwater interface in the marine clay layer might not be in equilibrium with the current hydrologic conditions in the upper glacial, but still responding to an equilibrium shift that occurred in the recent past.

It should be noted that the steady-state condition of the transient models was determined using plots of the head levels over time; stable head levels implied steady-state flow conditions. However, the transport portion of the model was in steady-state only when concentrations did not change over time. For this study, it was assumed that salt concentrations achieved steady-state in parallel with the flow portion of the model because flow and transport were coupled within a single time-step lag. Assuming there was no conceptual error in the model, this assumption should be appropriate. This is important because, although the calibration process focused on head levels, in the predictive modeling, the salt concentrations and position of the freshwater/saltwater interface were of primary interest.

A closely related assumption in this study was to ignore any effects of nutrient loading and transport within the model. Simmons (1986) found the various impurities in Shelter Island groundwater to be small compared to the overall solute concentration of seawater such that assuming the freshwater to have a concentration of zero introduced minimal error. However, it is possible that localized groundwater pollution could create a solute concentration high enough to noticeably effect the density relationship between the freshwater and groundwater and thereby cause deviation from the modeled simulations.

From Figure 24, which shows the flow lines within the freshwater lens, it appears that most recharge to Shelter Island leaves the aquifer as submarine groundwater

discharge. The model results are in general agreement with previous work by O'Rourke (2000) and Paulsen et al. (2004) that found below sea level seepage faces near the shoreline, often visible at low tide, which were responsible for most of the discharge of the aquifer. Although the region of discharge was confirmed in the SEAWAT-2000 model, it was more difficult to make any comparison of quantity of discharge with previous studies. Because submarine groundwater discharge is highly dependent on recharge, comparing discharge in different years or seasons is not meaningful.

The results shown in Figure 26 suggest that diffusion does not play a major role in the long-term movement of the freshwater/saltwater interface. This is a reasonable conclusion since molecular diffusion, as described by Fick's Law, is proportional to the concentration gradient and the velocity of the diffusive particles which is primarily dependent on temperature, particle size, and fluid viscosity (Domenico and Schwartz, 1998). Since none of these characteristics change within the model, it is assumed that diffusion is constant across all scenarios. However, because SEAWAT assumes constant temperature, it is possible that, due to global warming, the amount of diffusion at the freshwater/saltwater interface will increase over the next century because of an increase in temperature of the seawater and groundwater. Thus, it is not possible to make any realistic predictions regarding future diffusion without first estimating the future dispersion coefficient.

Lateral mechanical dispersion was not used in the simulations in this study. The model was two-dimensional and solute concentrations were assumed to be uniform perpendicular to the cross-section of model. When simulations were run with lateral

dispersion, the output confirmed that simplifying the model to exclude lateral dispersion was appropriate.

Tidal or seasonal mixing was not considered in this study. Paulson et al. (2004) found a daily asymmetrical change in submarine groundwater discharge and salinity. Thus, the range of brackish water is larger than that modeled when assuming a relatively stationary interface with a zone of diffusion. However, because this study was concerned with the long-term movement of the freshwater/saltwater interface, the daily and seasonal movement of the interface and the additional mixing it causes was not considered. In an October, 2007 Geological Society of America meeting, Motomu Ibaraki, of Ohio State University presented unpublished research that suggested that shores with highly sorted sandy layers may experience freshwater and saltwater mixing that causes saltwater intrusion 10% to 50% further inland than simple sea level rise inundation. If peer-review supports these findings, mixing may be an important component of future Shelter Island modeling.

Once the revised SEAWAT-2000 model was created and the calibration process began, it was clear that, although it was an improvement over the original Schubert (1999) model, weaknesses in the original carried over to the new model. The highest deviations from the field data occurred at the center of the island. This was attributed to that section of the model having the largest deviation from purely two dimensional flow (see Figure 7). Also, the observation closest to West Neck Bay, was substantially higher than the simulation. This was attributed to hydraulic tidal loading in the Schubert (1999) report. Schneider and Kruse (2003), in a study of a small sandy barrier island in Florida, found that tidal forcing caused water table elevations to change by several tens of

centimeters daily. Likewise, individual precipitation events could cause similar changes within days. Thus, estimating the freshwater/saltwater interface, which responds much more slowly over time, directly from any single set of head levels, yields uncertain results.

The predicted movement of the freshwater/saltwater interface agrees with the conceptual model of Simmons (1986). Because the marine clay unit restricts the movement of the bottom of the interface, the sides move substantially landward or seaward in response to hydrological conditions (see Figure 6). Since Simmons (1986) observed that the interface moves with the seasons and varying recharge, it is important to note that the model predicted movements of the freshwater/saltwater interface are long-term averages that would act as the new baseline from which regular season variability would fluctuate.

Because the model simulations did not consider surface topology and the few small near shore ponds on Shelter Island that intersect the water table, it is more difficult to determine the impact of scenarios 2 and 3 on the volume of freshwater under Shelter Island. If the effect of outflow to surface water is substantial, the actual head levels may be lower than simulated due to increased flow to ponds and subsequent higher evaporation rates. Additionally, by not considering surface topology, it was not possible to correctly model the horizontal movement of the shoreline that would occur as rising sea level inundated coastal land. On the northern shores of Shelter Island, where there are high bluffs rising from the shore, there should be minimal movement of the shoreline. At the southern end of Shelter Island, the movement of the shoreline may be more substantial and a source of error if not considered within the model. For the cross-section

modeled in this study (Figure 7), assuming a stationary shoreline simplified modeling while introducing an acceptably small error.

Conclusion

In order to quantify the effects that global warming may have on a small sandy barrier island, a previously published single density steady-state groundwater flow model for Shelter Island, NY was changed to a variable density transient groundwater flow model. The original model code, created for MODFLOW, was adapted to SEAWAT-2000 and run with PMWIN Pro as the graphical user interface. In order to obtain simulations that were consistent with field observations, the marine clay layer was set as a no-flow boundary in the SEAWAT-2000 model. The calibrated SEAWAT-2000 model had a variance of 0.38 compared to the original Schubert (1999) model variance of 0.47.

The 2007 IPCC report predictions for changes in precipitation and sea level rise over the next century were applied to the calibrated model. A scenario most favorable to groundwater retention consisting of a predicted precipitation increase of 15% and a sea level rise of 0.6 ft was compared to the current long-term average. This resulted in a seaward movement of the interface by an average of 76 ft and a maximum of 199 ft. The water table rose by an average of 0.89 feet. A second scenario least favorable to groundwater retention consisting of a predicted precipitation decrease of 2% and a sea level rise of 2 ft was compared to the current long-term average. This resulted in a landward movement of the interface by an average of 53 ft and a maximum of 121 ft. The water table rose by an average of 1.94 feet.

Future Work

Parameter estimation software usually fails due to either the insensitivity of the head observations, non-uniqueness of solutions, or model instability (Hill, 1998). In the case of this study, the limited head observations were a contributing factor to the failed automated parameter estimation. With an increased number of observation data, the chances of obtaining non-unique solutions would decrease significantly. Future modeling work should include increasing the number of observations to aid the calibration and validation process. Also, a redesigned model should use small uniform cell sizes both vertically and horizontally to minimize numerical instability issues. A model the island's aquifer in warmer climate should consider the effects of increased temperature on diffusion which presumably will increase the zone of diffusion at the freshwater/saltwater interface and further decrease the volume of potable water. Additionally, the effects of mixing on the brackish zone should be added to more precisely ascertain the extent of potable water.

In order to properly estimate the actual volumetric loss or gain of potable water on Shelter Island due to climate change over the next century, a full three-dimensional variable density flow model should be created that also incorporates the additional regional tectonic subsidence. Most importantly, the model should add surface topological features and include the intersection of ponds with the water table in order to model shoreline movement and to see what effects are caused by the increased evaporation and outflow resulting from a rising water table. Incorporating a water quality component to the model may also be necessary since one of the primary sources of contamination on Shelter Island is effluent from septic tanks. Because these sources are

closer to the water table than surface contaminants, a rising water table may cause a substantial increase in water pollution thereby further reducing the effective volume of potable water available to the residents of Shelter Island.

References

- Buxton, H.T., and Modica, E., Patterns and Rates of Ground-Water Flow on Long Island, New York, Ground Water , Vol. 30, No. 6, 857-866
- Chiang, Wen-Hsing, 2005, 3D-Groundwater Modeling with PMWIN, 2nd Edition, Heidelberg: Springer, 397 p.
- Christensen, J.H., B. Hewitson, A. Busuioc, A. Chen, X. Gao, I. Held, R. Jones, R.K. Kolli, W.-T. Kwon, R. Laprise, V. Magaña Rueda, L. Mearns, C.G. Menéndez, J. Räisänen, A. Rinke, A. Sarr and P. Whetton, 2007: Regional Climate Projections. In: Climate Change 2007: The Physical Science Basis. Contribution of Working Group I to the Fourth Assessment Report of the Intergovernmental Panel on Climate Change [Solomon, S., D. Qin, M. Manning, Z. Chen, M. Marquis, K.B. Averyt, M. Tignor and H.L. Miller (eds.)]. Cambridge University Press, Cambridge, United Kingdom and New York, NY, USA.
- Cohen, Philip, Franke, O.L., and Foxworthy, B.L., 1968, An atlas of Long Island's water resources: New York State Water Resources Commission Bulletin 62, 117 p.
- Davis, G.H., 1987, Land subsidence and sea level rise on the Atlantic Coastal Plain of the United States, Environmental Geology, Vol. 10, No. 2, p. 67-80
- Doherty, J. 1994, PEST: Corinda, Australia, Watermark Computing, 122 p.
- Domenico, P.A., 1972, Concepts and Models in Groundwater Hydrology, McGraw-Hill, New York, 405 p.
- Domenico, P.A. and Schwartz, F.W., 1998, Physical and Chemical Hydrogeology, 2nd Edition , New York: John Wiley & Sons, 494 p.
- Freeze, R. A., and Cherry, J. A., 1979, Groundwater: Englewood Cliffs, N.J., Prentice-Hall, 604 p.
- Fuller, M.L., 1914, The geology of Long Island, New York: U.S. Geological Survey Professional Paper 82, 231 p.
- Franke, O.L., and McClymonds, N.E., 1972, Summary of the hydrologic situation on Long Island, New York as a guide to water-management alternatives: U.S. Geological Survey Professional Paper 627-F, 59 p.
- Ghyben, W.B., 1889, Notes in verband met Woorgenomen Put boring Nabji Amsterdam, Tijdschr. Koninhitk, Inst. Ingrs., The Hague.

- Guo, Weixing, and Langevin, C.D., 2002, User's guide to SEAWAT: A computer program for simulation of three-dimensional variable-density ground-water flow: U.S. Geological Survey Techniques of Water-Resources Investigations, book 6, chap. A7, 77 p.
- Glover, R.E., 1959, The pattern of fresh-water flow in a confined coastal aquifer, *Journal of Geophysical Research*, Vol. 64, No.4, p.457-459
- Gornitz, V., 2000, Climate change and the coast: impacts in the New York City metropolitan region, *EOS*, Vol. 81, No.17, S73.
- Gornitz, V., Couch, S., and Hartig, E.K., Impacts of sea level rise in the New York City metropolitan area, *Global and Planetary Changes*, Vol. 32, p. 61– 88
- Herzberg, B., 1901, Die Wasserversovgung einiger Nordseebaser, *J. Gasbeleucht and wasserversov*, v. 44, p. 815-819
- Harbaugh AW, Banta ER, Hill MC and McDonald MG, 2000, MODFLOW-2000, The U.S. Geological Survey modular ground-water model User guide to modularization concepts and the ground-water flow process, U.S. Geological Survey Open-file report 00-92.
- Hill, M.C., 1998, Methods and guidelines for effective model calibration: U.S. Geological Survey Water-Resources Investigations Report 98-4005, 90 p.
- IPCC, Feb. 2007, *Climate Change 2007: The Physical Science Basis, Summary for Policymakers*, Contribution of Working Group I to the Fourth Assessment Report of the IPCC, Paris
- IPCC WGI, 2001, *Climate Change 2001: Scientific Basis*, Cambridge University Press, Cambridge
- Langevin, C.D., Shoemaker, W.B, and Guo, W., 2003, MODFLOW-2000, the U.S. Geological Survey Modular Ground-Water Model—Documentation of the SEAWAT-2000 Version with the Variable-Density Flow Process (VDF) and the Integrated MT3DMS Transport Process (IMT), U.S. Geological Survey Open-File Report 03-426
- Masterson, J.P., 2004, Simulated interaction between freshwater and saltwater and effects of ground-water pumping and sea-level change, Lower Cape Cod aquifer system, Massachusetts: U.S. Geological Survey Scientific Investigations Report 2004-5014, 72 p.
- Masterson, J.P. and Garabedian, S.P., Effects of Sea-Level Rise on Ground Water Flow in a Coastal Aquifer System, *Ground Water*, Vol. 45, No. 2, p. 209-217

- McDonald, M.G., and Harbaugh, A.W., 1984, A modular three-dimensional finite-difference ground-water flow model: U.S. Geological Survey Open-File Report 83-875, 528 p.
- McDonald, M.G., and Harbaugh, A.W., 1988, A modular three-dimensional finite-difference ground-water flow model: U.S. Geological Survey Techniques of Water-Resources Investigations, book 6, chap. A1, 586 p.
- Meehl, G.A., T.F. Stocker, W.D. Collins, P. Friedlingstein, A.T. Gaye, J.M. Gregory, A. Kitoh, R. Knutti, J.M. Murphy, A. Noda, S.C.B. Raper, I.G. Watterson, A.J. Weaver and Z.-C. Zhao, 2007: Global Climate Projections. In: *Climate Change 2007: The Physical Science Basis. Contribution of Working Group I to the Fourth Assessment Report of the Intergovernmental Panel on Climate Change* [Solomon, S., D. Qin, M. Manning, Z. Chen, M. Marquis, K.B. Averyt, M. Tignor and H.L. Miller (eds.)]. Cambridge University Press, Cambridge, United Kingdom and New York, NY, USA.
- Miller, J.F., and Rederick, R.H., 1969, The precipitation regime of Long Island, New York: U.S. Geol. Survey Prof. Paper 627-A, 21 p.
- Misut, P.E., and Feldman, S.M., 1996, Delineation of areas contributing recharge to wells in central Long Island, New York, by particle tracking: U.S. Geological Survey Open-File Report 95-703, 47 p.
- Misut, P.E., Schubert, C.E., Bova, R.G., and Colabufo, S.R., 2003, Simulated Effects of Pumping and Drought on Ground-Water Levels and the Freshwater-Saltwater Interface on the North Fork, Long Island, New York, U.S. Geological Survey Water-Resources Investigations Report 03-4184
- NAST, 2000, *Climate change Impacts on the United States: The potential consequences of climate variability and change*, US Global Change Research Program, Washington, DC
- Nemickas, B., and Koszalka, E. J., 1982, Geohydrologic appraisal of water resources of the South Fork, Long Island, New York: U.S. Geological Survey Water-Supply Paper 2073, 55 p.
- Nemickas, B., Mallard, G.E., and Reilly, T.E., 1989, Availability and historical development of ground-water resources of Long Island, New York—an introduction: U.S. Geological Survey Water-Resources Investigations Report 88-4113, 43 p.
- NSDWS, 2002, National Secondary Drinking Water Standards, Code of Federal Regulations (CFR), Title 40, Ch I, Part 143, Section 143.3
- NY GIS Clearinghouse, 2007, <http://www.nysgis.state.ny.us/>

- O'Rourke, D.E., 2000, Quantifying Specific Discharge into West Neck Bay, Shelter Island, New York Using a Three-Dimensional Finite-Difference Groundwater Flow Model and Continuous measurements with an Ultrasonic Seepage Meter, Masters Thesis, Stony Brook University
- Paulsen, R.J, O'Rourke, D, Smith, C.F and Wong, T.F., 2004, Tidal Load and Saltwater Influences on Submarine Ground Water Discharge, *Ground Water*, Vol. 42, No. 7, p 990-999
- Pearson, M., Taylor, J.Z., and Dingman, S.L., 1998, Sharp Interface models of Salt Water Intrusion and Wellhead Delineation on Nantucket Island, Massachusetts, *Ground Water*, Vol. 36, No. 5, p. 731-742
- Peltier, W.R., 1999, Global sea level rise and glacial isostatic adjustment, *Global and Planetary Change*, Vol. 20, p. 93–123
- Peterson, D.S., 1987, Ground-water recharge rates in Nassau and Suffolk Counties, New York: U.S. Geological Survey Water-Resources Investigations Report 86-4181, 19 p.
- Rummer Jr., R.R. and Shiau, J.C, 1968, Salt water interface in a layered coastal aquifer, *Water Resources Research*, Vol. 4, No. 6, p. 1235-1247
- Schneider, J.C. and Kruse, S.E., 2003, A comparison of controls on freshwater lens morphology of small carbonate and siliciclastic islands: examples from barrier islands in Florida, USA, *Journal of Hydrology*, Vol. 284, p. 253-269
- Schubert, C.E., 1998, Areas Contributing Ground Water to the Peconic Estuary, and Ground-water Budgets for the North and South Forks and Shelter Island, Eastern Suffolk County, New York, U.S. Geological Survey Water Resources Investigations Report 97-4136
- Schubert, C.E., 1999, Ground-Water Flow Paths and Traveltime to Three Small Embayments within the Peconic Estuary, Eastern Suffolk County, New York, USGS Water Resources Investigations Report 98-4181
- Schubert, C.E., Bova, R.G., and Misut, P.E., 2004, Hydrogeologic framework of the North Fork and surrounding areas, Long Island, New York: U.S. Geological Survey Water-Resources Investigations Report 02-4284, 4 sheets.
- Simmons, Dale L., 1986, Geohydrology and Ground-Water Quality on Shelter Island, Suffolk County, New York, 1983-84, U.S. Geological Survey Water-Resources Investigations Report 85-4165, 39 p.
- Smolensky, D.A, Buxton, H.T., and Shernoff, P.K., 1989, Hydrologic framework of Long Island, New York: U.S. Geological Survey Hydrologic Investigations Atlas HA-709, 3 sheets, scale 1:250,000.

- Soren, Julian, 1978, Hydrogeologic Conditions in the Town of Shelter Island, Suffolk County, Long Island, New York, U.S. Geological Survey Water-Resources Investigations Report 77-77, 22 p.
- Steenhius, T.S., Jackson, C.D., Kung, S.K.J., and Brutsaert, W., 1985, Measurement of groundwater recharge on eastern Long Island, New York, USA: Journal of Hydrology, v. 79, p. 145-169.
- Tiruneh, N.D. and Motz, L.H., 2003, Three Dimensional Modeling of Saltwater Intrusion Coupled with the Impact of Climate Change and Pumping, World Water Environ. Resour. Congr., ASCE, Philadelphia, p 1079-1087
- Titus, J.G. and Narayanan, V.K., 1995, The Probability of Sea level Rise, EPA, Washington D.C.
- Urbano, L.D, 2001, "The Impact of Climatic Change on Ground Water Systems." Diss. U of Minnesota
- Veatch, A.C., Slichter, C.S., Bowman, Isaiah, Crosby, W.O., and Horton, R.E., 1906, Underground water resources of Long Island, New York: U.S. Geological Survey Professional Paper 44, 394 p.
- World Meteorological Organization, 2005, Saving Paradise, Ensuring Sustainable Development, Small Island Developing States, WMO-No. 973
- Zheng, Chunmiao, and Wang, P.P., 1999, MT3DMS—A modular three-dimensional multispecies transport model for simulation of advection, dispersion and chemical reactions of contaminants in ground-water systems; documentation and user's guide: Jacksonville, Fla., U.S. Army Corps of Engineers Contract Report SERDP-99-1.

Appendix 1

Annual, seasonal, and long-term precipitation at Bridgehampton, Greenport, and Riverhead, Suffolk County, N.Y., and corresponding recharge from land surface and lakes, 1955-99 (Misult et al., 2004)

[Precipitation values are in inches. Boldface values are means for multiple years. --, no data available. Locations are shown in fig. 1.]

Station	Period ^a	Precipitation					Calculated recharge	
		Calendar year		October 15 through May 15			Land	Lakes
		Total	50 percent of total	Total	75 percent of total	90 percent of total		
BRIDGEHAMPTON	1955	43.26	21.63	26.10	19.58	23.49	21.53	9.56
	1956	45.27	22.64	32.25	24.19	29.03	26.61	11.57
	1957	35.79	17.90	22.87	17.15	20.58	18.87	2.09
	1955-57 mean	41.44	20.72	27.07	20.31	24.37	22.34	7.74
	1962	46.61	23.31	25.61	19.21	23.05	21.13	12.91
	1963	38.23	19.12	22.74	17.06	20.47	18.76	4.53
	1964	38.16	19.08	29.49	22.12	26.54	24.33	4.46
	1965	30.67	15.34	25.04	18.78	22.54	20.66	-3.03
	1966	37.28	18.64	15.23	11.42	13.71	12.56	3.58
	1962-66 mean	38.19	19.10	23.62	17.72	21.26	19.49	4.49
	1992	45.11	22.56	20.36	15.27	18.32	16.80	11.41
	1993	45.46	22.73	30.56	22.92	27.50	25.21	11.76
	1994	47.97	23.99	35.43	26.57	31.89	29.23	14.27
	1992-94 mean	46.18	23.09	28.78	21.59	25.91	23.75	12.48
	1996	67.54	33.77	36.95	27.71	33.26	30.48	33.84
	1997	47.47	23.74	36.19	27.14	32.57	29.86	13.77
	1998	55.79	27.90	47.63	35.72	42.87	39.29	22.09
	1996-98 mean	56.93	28.47	40.26	30.19	36.23	33.21	23.23
	1959-99 mean	46.08	23.04	28.81	21.61	25.93	23.77	12.38
GREENPORT	^b 1955-57 mean	--	--	--	18.69	22.43	20.56	7.01
	1962	42.03	21.02	21.46	16.10	19.31	17.70	8.33
	1963	35.34	17.67	20.68	15.51	18.61	17.06	1.64
	1964	44.31	22.16	26.95	20.21	24.26	22.23	10.61
	1965	25.94	12.97	21.33	16.00	19.20	17.60	-7.76
	1966	36.63	18.32	16.25	12.19	14.63	13.41	2.93
	1962-66 mean	36.85	18.43	21.33	16.00	19.20	17.60	3.15
	1992	43.82	21.91	20.82	15.62	18.74	17.18	10.12
	1993	42.34	21.17	27.39	20.54	24.65	22.60	8.64
	^c 1994	33.07	16.54	24.11	18.08	21.70	19.89	-0.63
	1992-94 mean	39.74	19.87	24.11	18.08	21.70	19.89	6.04
	1996	56.39	28.20	34.04	25.53	30.64	28.08	22.69
	^c 1997	35.16	17.58	30.10	22.58	27.09	24.83	1.46
	^b 1998	--	--	--	--	--	36.17	20.01
	1996-98 mean	45.78	22.89	32.07	24.05	28.86	29.70	14.72
1959-99 mean	44.91	22.46	26.52	19.89	23.87	21.88	11.21	
RIVERHEAD	1955	40.92	20.46	24.55	18.41	22.10	20.25	7.22
	1956	44.64	22.32	31.11	23.33	28.00	25.67	10.94
	^c 1957	43.15	21.58	23.89	17.92	21.50	19.71	9.45
	1955-57 mean	42.90	21.45	26.52	19.89	23.87	21.88	9.20
	1962	45.03	22.52	23.48	17.61	21.13	19.37	11.33
	1963	36.09	18.05	22.13	16.60	19.92	18.26	2.39
	1964	41.31	20.66	28.92	21.69	26.03	23.86	7.61
	1965	33.71	16.86	24.99	18.74	22.49	20.62	0.01
	1966	36.71	18.36	14.37	10.78	12.93	11.86	3.01
	1962-66 mean	38.57	19.29	22.78	17.08	20.50	18.79	4.87
	1992	45.09	22.55	17.22	12.92	15.50	14.21	11.39
	1993	45.58	22.79	28.85	21.64	25.97	23.80	11.88
	1994	42.51	21.26	31.41	23.56	28.27	25.91	8.81
	1992-94 mean	44.39	22.20	25.83	19.37	23.24	21.31	10.69
	1996	57.46	28.73	32.76	24.57	29.48	27.03	23.76
	1997	38.38	19.19	33.20	24.90	29.88	27.39	4.68
	^c 1998	52.66	26.33	42.47	31.85	38.22	35.04	18.96
1996-98 mean	49.50	24.75	36.14	27.11	32.53	29.82	15.80	
1959-99 mean	45.33	22.66	27.12	20.34	24.41	22.37	11.63	

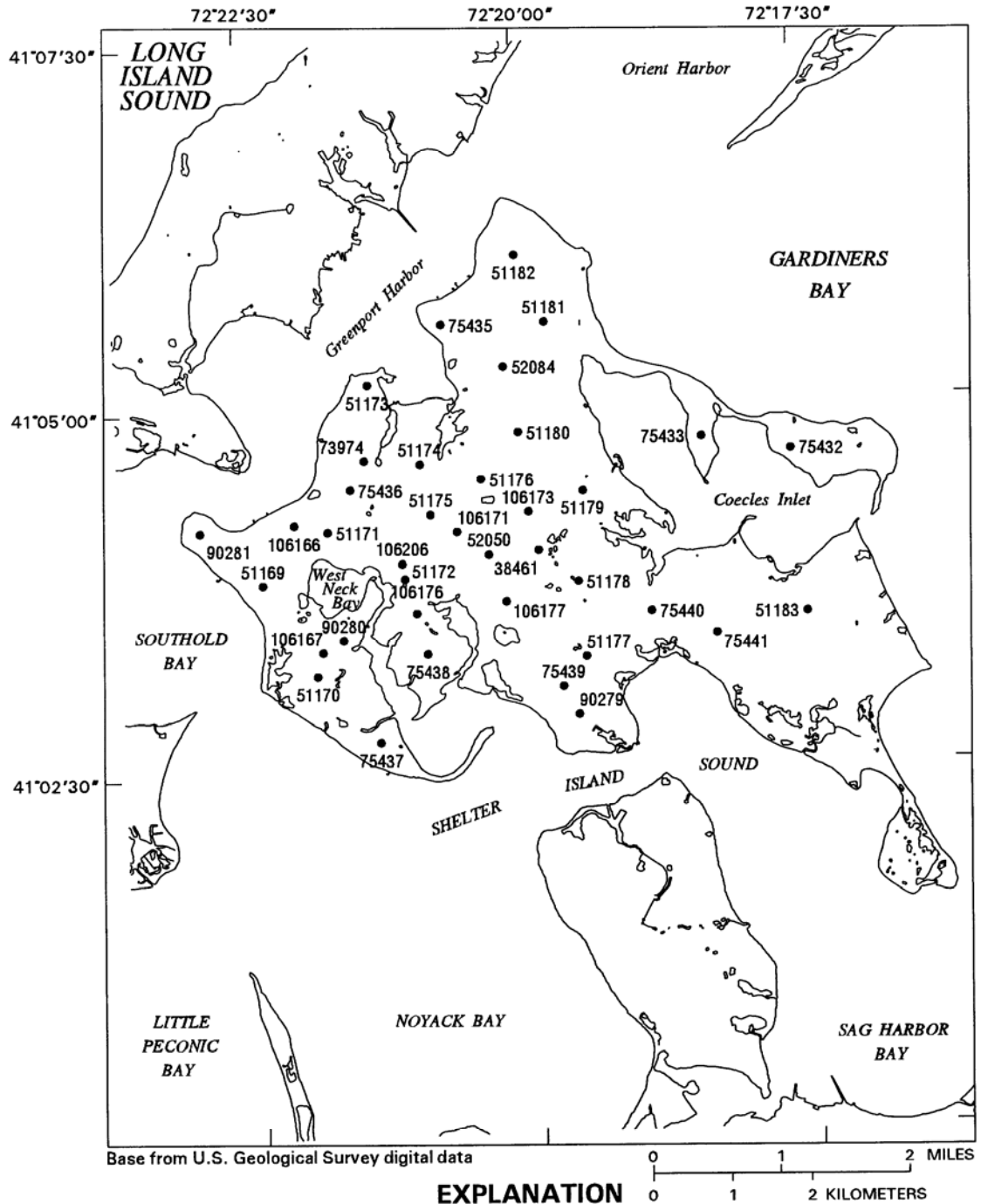
^a Long-term precipitation data incomplete for 1 or more years; data for those years were not used to compute long-term mean value.

^b Greenport recharge data for 1955-57 and 1998 estimated from Bridgehampton records and from the ratio of 1959-99 values.

^c Precipitation data for the following years and stations were unavailable; annual values for the stated months were estimated from Bridgehampton records: Greenport - September 1994 and October 1997. Riverhead - September 1957 and April 1998.

Appendix 2

Map of monitoring wells installed on Shelter Island installed for various studies (Soren, 1978) (Simmon, 1986) (Schubert, 1998) and data collected by the Suffolk County Department of Health for wells used to calibrate/validate the model in this study.



• 51183 OBSERVATION WELL -- Well measured in March 1995. Number is assigned by New York State Department of Environmental Conservation. Prefix "S" denoting Suffolk County is omitted.

(modified from Schubert, 1998)